REGIONAL SCALE EVAPORATION AND THE ATMOSPHERIC BOUNDARY LAYER

Marc B. Parlange
William E. Eichinger[1]
John D. Albertson
Hydrologic Science, University of California, Davis

Abstract. Evaporation into the atmosphere is fundamental to the fields of hydrology, meteorology, and climatology. With evolving interest in regional and global hydrologic processes there is an increasing recognition of the importance of the study of evaporation and land surface water balances for length scales of the order of 10 km. To obtain regional scale fluxes of water vapor, heat, and momentum, it is important to understand transport in the atmospheric boundary layer (ABL), which is defined to be that part of the atmosphere directly influenced by the land surface. In this review we briefly summarize some current models of evaporation and the ABL and discuss new experimental and computational opportunities that may aid our understanding of evaporation at these larger scales. In particular, consideration is given to remote sensing of the atmosphere, computational fluid dynamics and the role numerical models can play in understanding land-atmosphere interaction. These powerful modeling and measurement tools are allowing us to visualize and study spatial and temporal scales previously untouched, thereby increasing the opportunities to improve our understanding of land-atmosphere interaction.

1. INTRODUCTION

1.1. Evaporation in Hydrology

Our ability to describe hydrologic processes near the Earth's surface is dependent on our understanding of evaporation of water into the atmosphere. The errors involved in estimating evaporation can be as large as the individual subsurface transport components of the hydrologic budget. The hydrologic balance for a layer of soil at the land surface can be written

$$P = E + \Delta SW + q_r + q_s + q_d \qquad (1)$$

where P is precipitation, E is evaporation, ΔSW represents changes in the stored water in the soil layer, q_r is the net runoff rate over the soil surface, q_s is the net lateral subsurface flow, and q_d is the subsurface drainage at a lower boundary z_h. Each component of the hydrologic balance is integral to the understanding and description of the hydrologic system as a whole. Accordingly, all of these components are focused areas of intense research which depend ultimately on the evaporation history following precipitation events. In brief, infiltration into and water movement through the vadose zone, or unsaturated near-surface soil region, have been prime areas of interest to those concerned with problems of soil physics, solute transport, and erosion processes [e.g., *Parlange*, 1980; *Parlange et al.*, 1982; *Parlange et al.*, 1992b, 1993b; *Govindaraju et al.*, 1990; *Govindaraju and Kavvas*, 1991; *Hairsine and Rose*, 1992a, b; *Schmugge et al.*, 1994]. Hillslope subsurface and overland flow and soil moisture change is important in watershed description, especially during and following rainfall events [e.g., *Loague and Freeze*, 1985; *Parlange et al.*, 1989; *Wood et al.*, 1990; *Hornberger et al.*, 1991; *Stagnitti et al.*, 1992; *Sanford et al.*, 1993; *Troch et al.*, 1993; *Brutsaert*, 1994]. A great deal of work in hydrology has focused on the statistical properties of rainfall for hydrologic simulation, since precipitation is the largest term in the hydrologic balance [e.g., *Todorovic and Woolhiser*, 1975; *Katz*, 1977a, b; *Foufoula-Georgiou and Guttorp*, 1986; *Smith*, 1987; *Obeysekera et al.*, 1987; *Rodriguez-Iturbe et al.*, 1987; *Kavvas and Chen*, 1989; *Wilks*, 1993; *Woolhiser et al.*, 1993; *Katz and Parlange*, 1993, 1995; *Barros*, 1994].

Perhaps the least amount of effort on the part of the surface hydrology community has concerned the description, determination, and measurement of evaporation at catchment scales. This is surprising, since approximately two thirds of the precipitation over land surfaces is soon lost to evaporation [*Brutsaert*, 1982, 1986, 1991]. From the perspective of soil moisture

[1]Also at Los Alamos National Laboratory, Los Alamos, New Mexico.

Reviews of Geophysics, 33, 1 / *February 1995*
pages 99–124
Paper number 94RG03112

8755-1209/95/94RG-03112$15.00

TABLE 1. Values of the Parameters for Different Versions of (2) [*Crago and Brutsaert*, 1992]

Source	E	γ'	A	B
Wet surface [*Penman*, 1948]	E_p	γ	1	1
Equilibrium evaporation [*Slatyer and McIlroy*, 1967]	E_e	γ	1	0
Priestley and Taylor [1972]	E_{pt}	γ	α	0
Advection aridity [*Brutsaert and Stricker*, 1979]	E_{aa}	γ	$(2\alpha - 1)$	-1
Modified Penman-Monteith [*Thom*, 1972]	E_{pm}	$\gamma(1 + r_s cf(u)p/\rho)$	1	1

Here, r_s is a bulk surface resistance, c is a constant, p is the air pressure, and ρ is the average air density.

changes, evaporation represents a low-frequency forcing relative to precipitation influx [*Eagleson*, 1986; *Parlange et al.*, 1992a]. There is also evidence that the runoff is highly correlated to the antecedent soil moisture conditions and thus the evaporation [e.g., *Hewlett et al.*, 1977; *Loague and Freeze*, 1985; *Goodrich et al.*, 1994]. In short, our motivation is that an improved understanding of evaporation and further advances in the estimation and measurement of evaporative fluxes should logically result in significant improvements in our ability to model catchment responses to precipitation [*Stricker and Brutsaert*, 1978; *Burges*, 1986; *Goodrich et al.*, 1994].

1.2. Formulation of Evaporation Models

There is no agreement, in hydrologic practice, on a standard approach for the measurement of evaporation nor on a methodology for areal averaging. There are a number of evaporation equations in common use for the estimation of potential and actual evaporation. These formulations include those by *Penman* [1948], *Slatyer and McIlroy* [1967], *Priestley and Taylor* [1972], Penman-Monteith [*Monteith*, 1965], the Thom formulation of Penman-Monteith [*Thom*, 1972], and the advection-aridity approach of *Brutsaert and Stricker* [1979] based upon the *Bouchet* [1963] hypothesis. Related to the advection-aridity model [*Brutsaert and Stricker*, 1979; *Parlange and Katul*, 1992a] is the complementary model of *Morton* [1983] (see also *Granger* [1989]), which is also based upon the Bouchet hypothesis. All of these approaches have some basis in theory with one or more experimentally determined or estimated parameters. The common thread linking these models is their focus on the energy balance at the Earth's surface, where the net solar radiation incident on the surface, R_n, is divided among soil heat flux G into the ground, sensible heat flux H back to the atmosphere, and finally the latent heat flux L_eE into the atmosphere due to evaporation. These models differ in their bases for partitioning the available energy. The various equations can be expressed in the following general form:

$$L_eE = \beta\left[A\,\frac{\Delta}{\Delta + \gamma'}\,(R_n - G) + B\,\frac{\gamma}{\Delta + \gamma'}\,f(u)(e_a^* - e_a)\right] \tag{2}$$

where L_eE is the latent heat flux in watts per square meter; L_e is the latent heat of vaporization; E is the evaporation rate; Δ is the slope of the saturation vapor pressure curve taken at the temperature of interest; e and e^* are the vapor pressure and saturation vapor pressure of the air at some height above the surface, respectively; and γ represents the ratio of the specific heat of air at constant pressure to the latent heat of vaporization (generally taken to be a constant of 0.67 mbar/K at standard temperature and pressure). The function $f(u)$ is some function of the wind velocity, historically taken to be of the linear form $f(u) = a + bu$, with a and b being constants. A, B, β, and γ' are parameters which take on various values depending on the particular formulation (see Table 1). Note that β is the Budyko-Thornwaite-Mather parameter, which is defined as some function of the availability of surface water and is generally taken to be 1.0 until some measure of field capacity is reached and then allowed to decrease to zero with limited water availability [see *Crago and Brutsaert*, 1992].

These formulations are commonly used to give daily estimates of evaporation with a considerable degree of success when applied locally [e.g., *Stricker and Brutsaert*, 1978; *Crago and Brutsaert*, 1992]. Evaporation information at watershed or field scales is also useful in obtaining field scale effective soil hydraulic parameters by way of inverse techniques [e.g., *Bouttier et al.*, 1993; *Parlange et al.*, 1992a, 1993a]. When short term estimates are required, the effect of atmospheric stability is important and must be considered [*Stricker and Brutsaert*, 1978; *Brutsaert*, 1982; *Katul and Parlange*, 1992; *Parlange and Katul*, 1992b; *Mahrt and Ek*, 1993]. A wide variety of studies, such as the modeling of watersheds, regional landscape management, flood prediction, or climate change mod-

eling, require the measurement or parameterization of evaporation over a large area. While these models of evaporation have been used in many studies, they have been less successful when applied regionally or at the catchment scale. A major stumbling block is that we are unable to independently evaluate a priori the effective regional values of the free parameters in these equations (such as the surface resistance or β) [*Carson*, 1982; *Brutsaert*, 1986, 1991]. One serious difficulty, for example, is the estimation of soil moisture content and soil-plant-atmosphere relations over a large region in order to estimate β, since these properties are known to vary considerably over short distances [*Nielsen et al.*, 1973; *Goutorbe et al.*, 1989; *Vandervaere et al.*, 1994]. Relative to this, so-called effective surface resistance properties are difficult to estimate in a meaningful sense at desired scales for naturally heterogenous land surfaces. The development of surface resistance schemes in hydrology and atmospheric science is being driven, in a large part, by the need for land surface parameterizations for simulation in general circulation models (GCMs) or mesoscale models [e.g., *Skukla and Mintz*, 1982; Dickinson, 1984; *Dickinson et al.*, 1993; *Sellers et al.*, 1986; *Avissar and Pielke*, 1989; *Noilhan and Planton*, 1989; *Bougeault et al.*, 1991; *Seth et al.*, 1994]. As the present paper addresses the estimation of regional scale evaporation, the reader interested in land surface parameterization for climate modeling is referred to some previous papers in *Reviews of Geophysics* [see *Avissar and Verstraete*, 1990; *Wood*, 1991].

One way to approach the problem of estimating regional scale evaporation is to capitalize on the great disparity between the horizontal length scale of surface inhomogeneities and the horizontal length scale of the turbulent flows in the atmospheric boundary layer (ABL); these length scales are typically orders of magnitude apart. The horizontal length scale of the ABL can be described by its relation to the depth of the daytime ABL, which we know to be of the order of 1 km. The effect of the surface fluxes on the ABL moves vertically at a rate similar to the turbulent vertical wind speed fluctuations, while the effect of the surface fluxes is advected downwind at about the mean wind speed [*Tennekes and Lumley*, 1972, p. 16]. What is more, the turbulent nature of the vertical movement causes a great uncertainty in parcel travel time as the flow is rapidly mixed. This causes a parcel near the top of the ABL to be related to upwind surface fluxes spread over ~10 km. So, in effect, this scale disparity and the turbulent mixing work to average or smooth over the surface inhomogeneities. *Brutsaert* [1982, 1986, 1991] has discussed this point and advocated the use of large-scale ABL parameterizations that account for the turbulent mixing in a way that allows for the estimation of evaporation without having to deal with the details of the soil or surface vegetation characteristics. The past decade or two have seen extensive experimental work on this problem [e.g., *Lindroth*, 1984; *André et al.*, 1986, 1988, 1989; *Brutsaert and Kustas*, 1985; *Kustas and Brutsaert*, 1987; *Hacker*, 1988; *Hogstrom*, 1988; *Kader*, 1988; *Kader and Perepelkin*, 1989; *Brutsaert et al.*, 1990; *Betts et al.*, 1990; *Tsvang et al.*, 1991; *Eloranta and Forrest*, 1992; *Brutsaert and Sugita*, 1992a, b, c; *Noilhan et al.*, 1991; *Sugita and Brutsaert*, 1991; *Sellers et al.*, 1992; *Brutsaert and Parlange*, 1992; *Betts*, 1992; *Schols and Eloranta*, 1992; *Parlange and Brutsaert*, 1993; *Nichols and Cuenca*, 1993; *Mahrt and Ek*, 1993; *Bolle et al.*, 1993; *Stannard et al.*, 1994; *Kustas and Goodrich*, 1994; *Humes et al.*, 1994; *Parlange and Katul*, 1995].

The difficulty in developing a complete theoretical basis for regional evaporation and the ABL over complex terrain results from the fact that the Reynolds-averaged Navier-Stokes equations, which govern the mean flow, are not closed. With the lack of a complete theoretical basis, there is also the question of what parameters need to be measured (as opposed to the question of what parameters can be measured). Wind tunnels have been helpful in increasing our understanding of turbulent flow but are unable to capture the full complexity of flow at the scales of interest in nature. If we are to improve our understanding of evaporation at the scale of the watershed or river basin, we must study the processes from measurements made at the scales of interest. Over the past 10 years there has been a continually increasing effort to organize field experiments that make measurements in the ABL as well as on the surface as a means of revealing processes of the hydrologic physics at the larger scales. These experiments include the Hydrologic-Atmospheric Pilot Experiment–Modélisation du Bilan Hydrique (HAPEX-MOBILHY) [*André et al.*, 1986, 1988, 1989; *Goutorbe et al.*, 1989; *Noilhan et al.*, 1991], HAPEX-Sahel, First International Satellite Land Surface Climatology Project (ISLSCP) Field Experiment (FIFE) [*Sellers et al.*, 1992], Monsoon '90 [*Kustas and Goodrich*, 1994], the Northern Wetlands Study (NOWES) [*Glooschenko et al.*, 1994], the European Field Experiment in Desertification-Threatened Areas (EFEDA) [*Bolle et al.*, 1993; *Vandervaere et al.*, 1994] and the Boreal Ecosystem Atmosphere Study (BOREAS).

Many of the field experiments have incorporated mesoscale numerical models in their planning and execution to optimize the siting and deployment of instruments [e.g., *André et al.*, 1986, 1988]. In this way these models allow us to anticipate probable events or effects and set out to measure them with precision, thus making these experiments far more effective in accomplishing their goal of areal evaporation measurement. Many of these experiments have also incorporated remote-sensing field instruments capable of making detailed measurements of land surface [see *Choudhury*, 1991] and atmospheric properties over long distances. The atmospheric probing instruments are helping to improve our understanding of the atmo-

sphere, especially the spatial characteristics of the ABL. While there is no substitute for testing new concepts in actual field experiments, we also need ways to gain further insight without necessarily carrying out complete field experiments. The use of computer models allows us to do just that: to test and isolate ideas and theories in a convenient and straightforward manner. In particular, large eddy simulation is providing opportunities to "visualize," in three dimensions, ABL turbulent transport through time.

In this review we focus on efforts made to understand regional scale hydrologic phenomena through improved descriptions of the ABL. We begin this effort with a discussion of similarity theory, which has been successfully applied over near ideal and even more complex terrain to solve for surface fluxes (sections 2 and 3). As we look to the future for improvements to our understanding of ABL flow and transport, we are faced with the question of how to acquire the information to support model development and testing. The answer will certainly contain a balance of numerical simulation and field experimentation over the scales of interest. Therefore we follow the discussion of similarity theory with an introduction to large eddy simulation (LES) (section 4), and close with a review of remote sensing instrumentation and some techniques being used to probe the ABL to obtain spatial-temporal turbulent scaling information (section 5).

2. THE ATMOSPHERIC BOUNDARY LAYER

2.1. The Structure of the Boundary Layer

To begin to describe evaporation at the scales of interest in hydrology, it is important to understand the structure and dynamics of the ABL, which is defined as that portion of the atmosphere directly influenced by the land surface. This importance is due to the crucial integrative role that the ABL plays in combining the spatially variable surface fluxes at regional scales, given the complex terrain and surface properties found in most watersheds and river basins.

A schematic of the convective ABL is presented in Figure 1. A convective ABL occurs during daylight hours when solar heating warms the surface, allowing for convectivly driven turbulence. Typically, turbulent boundary layers have vertical to horizontal scale ratios of about 1:10 to 1:100, such that at a point along the flow the ABL characteristics could represent the impact of surface flux conditions over upwind distances of 10 km or more [*Sugita and Brutsaert*, 1990a, 1991; 1992a; *Brutsaert and Parlange*, 1992]. Above the ABL lies the free atmosphere, which is not immediately influenced by the presence of the surface. The surface layer is assumed to be affected mainly by the surface fluxes, while the mixed layer is more strongly impacted by boundary layer entrainment of the free atmosphere. A manifestation of this is shown schematically in Figure 1, where the potential temperature and specific humidity profiles in the outer region appear dissimilar owing to the entrainment of the relatively warm-dry air from above. The roughness wake layer is the lowest part of the ABL, below the blending height, where local scale roughness and heating characteristics are significant (i.e., close enough to the surface that the turbulence is unable to fully integrate over the inhomogeneities).

2.2. The Atmospheric Surface Layer

The atmospheric surface layer occupies about the lowest 10% of the fully developed daytime ABL, or the first 100 m or so above the Earth's surface. This is, for logistical reasons, the simplest part of the atmosphere in which to carry out regular measurements and has historically been the subject of the majority of field investigations (compared, for example, with mixed layer flows). Most studies of the atmospheric surface layer have been carried out over flat, uniform surfaces. These studies have laid the foundation for more recent studies of flow over the more realistic rugged and complex terrain [see *Kaimal and Finnigan*, 1994; *Kustas and Goodrich*, 1994]. Flow of air in the atmosphere, with its diurnal cycle and relationship to the land below, is nonsteady and horizontally inhomogeneous. The assumptions of steady, horizontally homogeneous flow, which are implicit to Monin-Obukhov similarity theory [*Monin and Obukhov*, 1954] are nonetheless considered applicable because of the large ratio of vertical to horizontal gradients of the observed mean scalar concentrations and wind speed, over averaging times of 10 min to about 1 hour. Furthermore, the surface layer of the ABL is not normally affected significantly by entrainment at the ABL capping inversion [*André et al.*, 1979; *Artaz and André*, 1980].

2.2.1. Surface layer under neutral atmospheric stability. To begin to describe the surface layer, we first consider the simplest situation: where the wind is brisk and there exist clouds which limit the solar radiation reaching the Earth's surface. In this case, buoyancy forces due to density stratification are negligible and the well known logarithmic wind profile

$$V = \frac{u_*}{k} \ln\left(\frac{z - d_0}{z_0}\right) \tag{3}$$

is appropriate to describe the vertical profile of the mean wind speed V. Here $u_*(=(\tau_0/\rho)^{1/2})$ is the friction velocity, τ_0 is the surface shear stress, ρ is the density of the air, k (= 0.4) is the von Kármán constant, z is the height above the ground, z_0 is the surface roughness, and d_0 is the momentum displacement height. The flux of momentum (τ_0) is critical to the quantification of the flux of water vapor away from the land surface; in this context it becomes essential to obtain the surface shear stress for evaporation model-

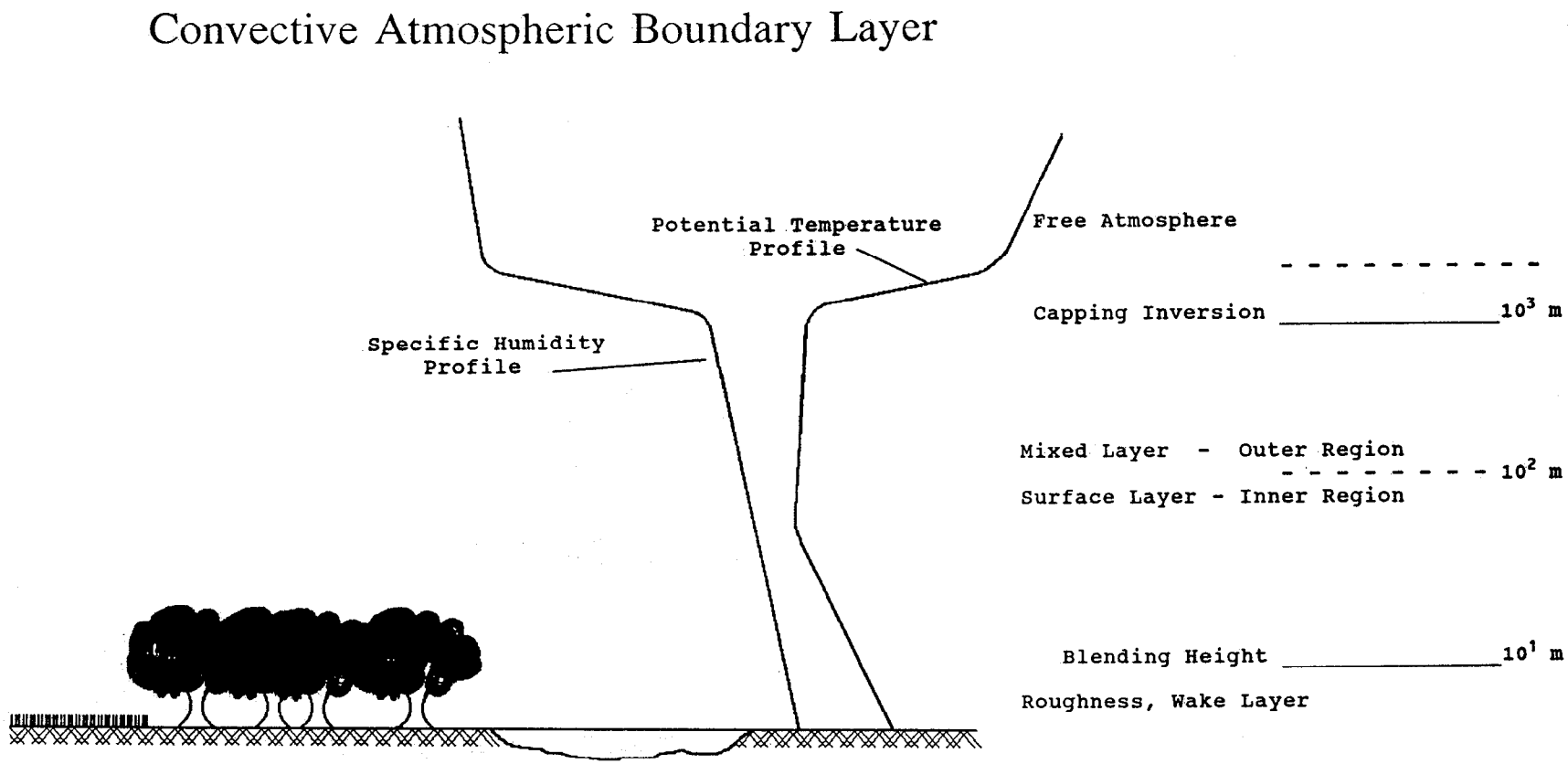

Figure 1. A schematic of the convective atmospheric boundary layer showing typical heights for the various components. A major practical problem is that most theories require a uniform surface. Most real surfaces are even more complex than shown here, containing differences in soils and surface altitudes.

ing. Equation (3) is used to derive z_0, or, less frequently, to derive d_0. The natural log of the surface roughness represents the zero velocity intercept of the logarithmic wind profile as can be seen from simple rearrangement of (3),

$$\ln (z - d_0) = \frac{kV[z]}{u_*} + \ln (z_0) \tag{4}$$

so that wind profile measurements $V[z]$ under neutral atmospheric stability allow the determination of z_0. The surface roughness (z_0) for different surfaces is tabulated in various books [e.g., *Brutsaert*, 1982; *Panofsky and Dutton*, 1984; *Stull*, 1988; *Garratt*, 1992] and in the recent review paper by *Wieringa* [1993]. For generally simple surfaces, such as fields covered with agricultural crops, many estimates of z_0 have been obtained [e.g., *Businger et al.*, 1971]. There has been a heightened effort over the past several years to obtain values of z_0 for various field sites from wind profiles measured under neutral atmospheric stability. However, it is a nontrivial task, since true, steady state neutral atmospheric stability is rarely observed. Large errors in the estimate of z_0 can result from using horizontal wind speed profiles measured during the transition from stable atmospheric stability conditions in the morning to unstable daytime conditions when the vertical gradient of the potential temperature changes sign. Under these conditions one cannot assume that the properties of the atmosphere are constant during the course of the measurement, a necessary requirement for (3). Some surface roughness results obtained over complex terrain as part of large field experiments are now becoming available [e.g., *Kustas and Brutsaert*, 1986; *Parlange and Brutsaert*, 1989; *Brutsaert et al.*, 1989; *Sugita and Brutsaert*, 1990b; *Parlange and Katul*, 1995]. In most cases the wind profiles in the neutral surface layer were measured with radiosondes or tethersondes. In the Alpine Experiment (ALPEX) in the pre-Alps of Switzerland, largely covered by pasture and one-fourth forest, where the terrain consists of hills of the order of 100 m above the mean valley elevations with distances between ridges of the order of 1 km, *Kustas and Brutsaert* [1986] found $z_0 = 3.8$ m with a corresponding $d_0 = 46$ m. *Parlange and Brutsaert* [1989], during the HAPEX-MOBILHY field campaign, studied the Landes Forest region of southwestern France and found $z_0 = 1.2$ m and $d_0 = 6.0$ m. Similar results were obtained from sodar-derived wind profiles during the experiment [*Parlange and Brutsaert*, 1990]. With the value of z_0 estimated and u_* known, the evaporation under neutral atmospheric stability may be calculated from a similar logarithmic equation for the specific humidity q profile

$$q - q_r = \frac{-E}{ku_*\rho} \ln \left(\frac{z - d_{0v}}{z_r - d_{0v}} \right) \tag{5}$$

where q_r is the specific humidity at some (arbitrary) reference level z_r in the logarithmic layer and d_{0v} is the displacement height for water vapor. Although it is known that d_{0v} is not the same as d_0, they are normally assumed to be equivalent [*Brutsaert*, 1982]. If the instruments are placed well above the roughness wake layer (see Figure 1), the exact determination of this value becomes less important as $z \gg d_{0v}$. If the surface is wet, the surface specific humidity q_s can be calculated from the surface temperature T_s [see *Brutsaert et al.*, 1989]. Thus (5) can be written

$$q - q_s = \frac{-E}{ku_*\rho} \ln \left(\frac{z - d_{0v}}{z_{0v}} \right) \tag{6}$$

where z_{0v} is the scalar roughness length for water vapor (i.e., the height at which the extrapolated log profile intersects $q = q_s$ [*Brutsaert*, 1982]).

A similar expression can be written for the potential temperature θ profile

$$\theta - \theta_s = \frac{-H}{ku_*\rho C_p} \ln \left(\frac{z - d_{0h}}{z_{0h}} \right) \tag{7}$$

where H is the sensible heat flux, c_p is the specific heat at constant pressure, the subscript s refers to the surface, and z_{0h} and d_{0h} for temperature are often assumed to be equal to those for specific humidity. As the momentum and scalar displacement heights are typically assumed equal, we will now use a general d_0.

2.2.2. The surface layer with thermal stratification. Under unstable atmospheric conditions, typically during the day when the land surface is heated by solar radiation, Monin-Obukhov similarity theory [*Monin and Obukhov*, 1954] is found to give reasonable descriptions of the mean and variance quantities in the surface layer of the ABL. The important parameters are buoyancy (g/θ), the height above the surface (z), the friction velocity u_*, and the surface flux of virtual sensible heat ($H_v = H + 0.61T_a c_p E$); T_a is the air temperature near the ground. Monin-Obukhov similarity theory states simply that the various atmospheric measures (e.g., gradients, variance, and covariances) depend only on these parameters and can be written as universal functions of the stability parameter $(z - d_0)/L$; where L is the Obukhov length, defined by

$$L = -\frac{u_*^3}{kg[H_v/(\rho c_p T_a)]} \tag{8}$$

Note that $(z - d_0)/L$ is a ratio of buoyant to mechanical production of turbulent kinetic energy. Equations (3), (5), and (7) can be written for the influence of buoyancy as

$$V = \frac{u_*}{k} \left[\ln \left(\frac{z - d_0}{z_0} \right) - \psi_m \left(\frac{z - d_0}{L} \right) \right] \tag{9}$$

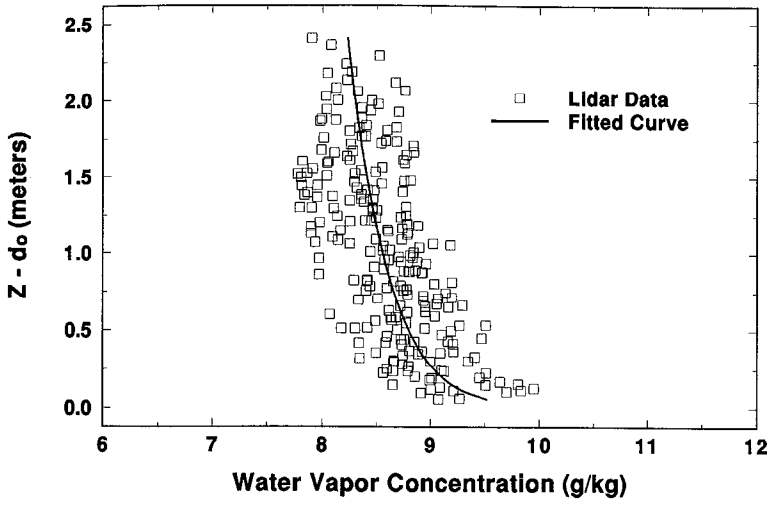

Figure 2. An example of the profile of water vapor concentration with height above the ground from August 23, 1991, taken over a bare soil field at the University of California, Davis. Also shown is the q profile from equation (11). While individual measurements may not conform exactly to the prediction, spatially or temporally averaged measurements show good agreement.

$$\theta_1 - \theta = \frac{H}{ku_*\rho c_p}\left[\ln\left(\frac{z-d_0}{z_1-d_0}\right) - \psi_t\left(\frac{z-d_0}{L}\right) + \psi_t\left(\frac{z_1-d_0}{L}\right)\right] \quad (10)$$

$$q_1 - q = \frac{E}{ku_*\rho}\left[\ln\left(\frac{z-d_0}{z_1-d_0}\right) - \psi_v\left(\frac{z-d_0}{L}\right) + \psi_v\left(\frac{z_1-d_0}{L}\right)\right] \quad (11)$$

where ψ_m, ψ_t, and ψ_v represent integral stability functions and z_1 is a reference height in the surface layer. The stability functions have been obtained experimentally [e.g., *Businger et al.*, 1971; *Dyer*, 1974; *Yaglom*, 1977; *Hogstrom*, 1988] and can be found in a number of texts on the subject [e.g., *Brutsaert*, 1982; *Panofsky and Dutton*, 1984; *Stull*, 1988; *Sorbjan*, 1989; *Garratt*, 1992]. Figure 2 is a comparison of (11) with data from a water vapor profile taken over an irrigated bare soil surface using a lidar. If profiles of V, q, and θ are measured, then the surface fluxes u_*, E, and H can be determined by iteratively using equations (8), (9), (10), and (11). Note that the stability functions for sensible heat and water vapor are generally assumed to be equal. This assumption is the basis of the well-known Bowen ratio–energy balance method.

This similarity scheme of *Monin and Obukhov* [1954] provides a good description of the mean profiles over uniform surfaces, the exception in nature. Until recently, much less has been known about the applicability of the surface layer similarity theory over rougher terrain. *Brutsaert and Kustas* [1985] measured surface layer profiles with radiosondes over the forealps of Switzerland and found the wind and humidity profiles to be well described by (9) and (11). More recently, in a reexamination of the data, *Qualls et al.* [1993] found the temperature profiles to be satisfactory as well. *Brutsaert and Sugita* [1990] and *Sugita and Brutsaert* [1990a, 1991] studied the ABL over the Flint hills of eastern Kansas and found that temperature and humidity profiles allowed reasonable estimates of the surface heat fluxes. If the surface temperature is known from remote thermal sensing, more reliable surface flux estimates may be obtained [*Sugita and Brutsaert*, 1990a, 1992b; *Brutsaert and Sugita*, 1992c]. Over the patchy Landes Forest in southwestern France, *Brutsaert and Parlange* [1992] found the profile-derived fluxes compared favorably with surface measurements over the forest [*Gash et al.*, 1989]. The wind profiles can also be satisfactorily modeled this way [*Parlange and Brutsaert*, 1993; *Tsvang et al.*, 1991] on the basis of comparisons with direct measurements of the friction velocity using eddy correlation techniques ($u_* = [-\langle u'w'\rangle]^{1/2}$, where u' is the fluctuating longitudinal wind speed, w' is the fluctuating vertical wind speed, and angle brackets represent the time averaging operator). *Parlange and Katul* [1995], in the Ojai Valley of southern California, found good agreement between direct measurements of friction velocity using a three-dimensional sonic anemometer and profile-derived estimates obtained from tethersondes.

In an interesting study, *Kader and Yaglom* [1990] reexamined and refined the formulation of similarity theory in the surface layer, drawing on theory due to *Zilitinkevich* [1971] and *Betchov and Yaglom* [1971] and using data collected over a 7-year period in Russia. Their theory is based upon directional dimensional analysis in which different length scales are used to characterize horizontal and vertical motions. Kader and Yaglom provided evidence for three sublayers: a "dynamic" sublayer, where the important scaling length is the horizontal and buoyancy effects are negligible; a "dynamic-convective" sublayer in which both horizontal and vertical motions become important and all of the flow parameters are relevant; and a "free convection" sublayer [*Tennekes*, 1970] where the vertical length is the important dimension, the

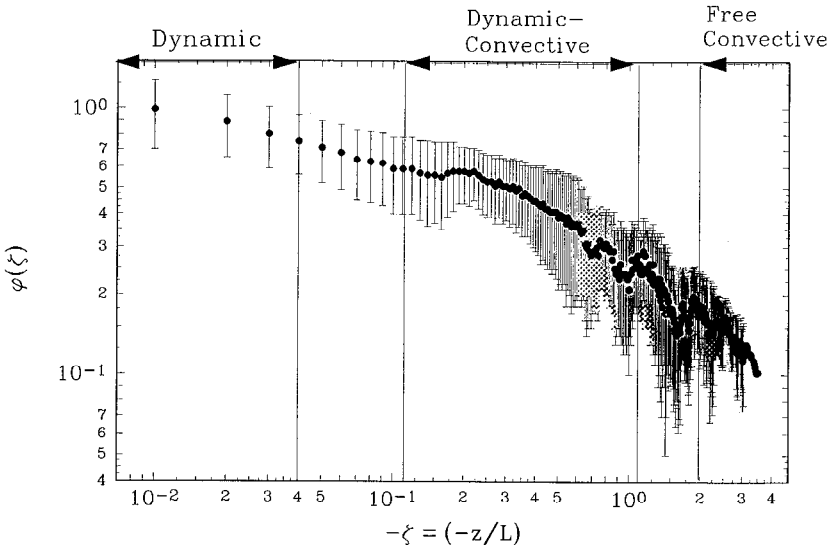

Figure 3. A plot of lidar-derived stability function for water vapor under convective (unstable) conditions. Also shown are the three surface sublayer regions predicted by *Kader and Yaglom* [1990]. The error bars represent the standard deviations of the measurements.

scaling velocity w_* is based on buoyancy, and u_* is not relevant. Additional data analysis of *Kader* [1988] and *Kader and Perepelkin* [1989] gave support to the concept of the three sublayers. Some evidence in support of the three sublayer model is presented in Figure 3, where profiles of ϕ_v, deduced from lidar measurements of q profiles, are shown plotted against the stability parameter ζ $(= z/L)$ (M. B. Parlange et al., Lidar measurements of the scalar similarity function in the unstably stratified turbulent atmosphere, submitted to *Boundary Layer Meteorology*, 1995; hereinafter Parlange et al., submitted manuscript, 1995); the q profiles were measured over a field at the University of California with a Raman lidar (see section 5.4), and ϕ_v is the gradient form of the integral function ψ_v. Though this may not have an immediate and direct impact on flux calculations, it is certainly important to our understanding of the lower atmospheric transport mechanisms and may support refinements of the stability correction functions and ultimately the estimation of evaporation in practice.

2.3. Structure Functions, Spectral Scaling, and Intermittency

The mechanisms by which scalars (primarily heat and water vapor, but also any pollutant or contaminant) are transported in a turbulent flow are still not well understood. To a large degree this is due to our incomplete understanding of turbulence in general. As an example, *Duncan and Schuepp* [1992], using measurements of CO_2 and water vapor from aircraft over the FIFE site, demonstrated that most of the flux was carried by a relatively small number of the convective structures. Another example is our emerging understanding of the role shear-driven structures play in surface-atmosphere exchange over rough canopies such as forest [*Shaw et al.*, 1989].

Basic investigations into the mechanisms responsible for turbulent transport often involve the study of statistics and spectral characteristics of the velocity and concentration variations [*Gibson and Schwartz*, 1963]. Although this review is not directed at local scale mechanisms, we mention some of the work here, as it promises to improve our understanding of the larger-scale problems as well.

Using the technique of conditional sampling [see *Antonia*, 1981] various groups have attempted to isolate the role of different structures in the transport of materials in the atmosphere [e.g., *Baldocchi and Meyers*, 1989; *Katul et al.*, 1994c]. Other techniques involve the use of structure functions and spectral transforms with *Kolmogorov*'s [1941] theory for scaling in the inertial subrange of high Reynolds number flows. Deviation from the Kolmogorov scaling has been noted in experiments studying higher-order structure functions [*Anselmet et al.*, 1984]; this deviation has classically been attributed to intermittency effects, as noted by Landau [*Landau and Lifshitz*, 1959]. Many phenomenological models for intermittency corrections to the 1941 Kolmogorov model include intermittency effects intrinsic to either the dissipation rate or fractallike buildup of intermittency during the energy cascade process [e.g., *Kraichnan*, 1991]. Examples of these phenomenological models include the lognormal model [*Kolmogorov*, 1962], the β model [*Frisch et al.*, 1978], and other multifractal models [*Meneveau and Sreenivasan*, 1987, 1991; *Aurell et al.*, 1992].

Studies of intermittency in ABL flows typically use Fourier power spectra and structure functions [e.g., *Mahrt*, 1989]. However, orthonormal wavelet transforms have recently been used to quantify intermittency effects on inertial subrange scaling of velocity, temperature, and humidity measurements in the surface layer [e.g., *Katul et al.*, 1994a, b; *Katul and Parlange*, 1994, 1995]. The wavelet technique is well suited to this work in that it unfolds the turbulent signal into scale and space, whereas the Fourier transform is space filling and therefore provides only scale

information. This is important because intermittent events, by definition, are active only at specific locations in the flow. These investigations are improving our understanding of the basic turbulence processes at local scales and are beginning to add insight to the larger-scale efforts.

3. SIMILARITY THEORY OF THE BULK ABL

The characteristic horizontal length scales of the atmosphere are typically orders of magnitude greater than those defining the land surface. Regional evaporation studies therefore may be less complicated when viewed from an ABL perspective. However, if the evaporative flux is to be estimated over length scales approaching tens of kilometers, and we recall the 1:10 to 1:100 ratio of vertical to horizontal scales in the ABL, it becomes necessary to study the entire ABL. Unfortunately, much less is known about the mixed layer than about the surface layer. Mixed layer flows have less sensitivity to the surface flux conditions and more dependence on entrainment fluxes [*Tennekes*, 1973] at the top of the ABL [*André et al.*, 1979; *Artaz and André*, 1980; *Wyngaard et al.*, 1984; *Wyngaard and Brost*, 1984]. Under convective conditions, which are of primary concern, the mixed layer is marked by large convective motions that scale with the depth of the boundary layer [*Mahrt*, 1976]. The mixed layer tends to warm uniformly with height, thus causing a steady decrease of H with z. This is in contrast to the surface layer, where the fluxes are approximately constant with height. An additional complication is introduced near the top of the mixed layer, as the entrainment of mass and energy becomes an important process. These differences between the surface and mixed layers give rise to similarity relationships that are somewhat different from those discussed for the surface layer. A great deal of effort has been invested in addressing the scaling of flow variables in the mixed layer, employing approaches such as mixed layer scaling and local similarity [e.g., *Sorbjan*, 1989; *Garratt*, 1992]. These approaches draw on dimensional parameters that are tailored to the mixed layer and typically do not apply to the surface layer. As our interest is in relating bulk boundary layer properties to surface fluxes, we will focus here on the extension of Monin-Obukhov similarity theory to the bulk ABL.

3.1. Extended Monin-Obukhov Similarity Theory

An extension of Monin-Obukhov similarity theory to include the mixed layer in addition to the surface layer yields a bulk transport formulation, which is analogous to the surface layer formulation and is based, in part, on the work of *Kazanskii and Monin* [1961], *Zilitinkevich and Deardorff* [1974], *Arya and Wyngaard* [1975], *Yamada* [1976], and *Brutsaert and Mawdsley* [1976]. For instance, the surface fluxes can be written as

$$E = ku_*\rho(q_1 - q_b) \cdot \left[\ln\left(\frac{h_b - d_0}{z_1 - d_0}\right) + \psi_v\left(\frac{z_1 - d_0}{L}\right) - D\right]^{-1} \tag{12}$$

$$u_* = k\langle V\rangle\left\{\left[\ln\left(\frac{h_b - d_0}{z_0}\right) - B\right]^2 + A^2\right\}^{-1/2} \tag{13}$$

$$H = ku_*\rho c_p(\theta_1 - \theta_b) \cdot \left[\ln\left(\frac{h_b - d_0}{z_1 - d_0}\right) + \psi_t\left(\frac{z_1 - d_0}{L}\right) - C\right]^{-1} \tag{14}$$

where A, B, C, and D are bulk similarity functions that account for parameters important in the mixed layer [*Brutsaert*, 1982], h_b is the depth of the boundary layer, subscript 1 denotes values at the lower measurement height, subscript b denotes the top of the boundary layer, $\langle V\rangle$ is taken as the mean resultant wind speed at the top of the boundary layer or average in the mixed layer, L remains the Obukhov length, and ψ_v and ψ_t are the surface layer stability correction functions [*Sugita and Brutsaert*, 1992a]. The estimation of E from (12) requires knowledge of u_* and H (for D). Unless independent momentum and heat flux information is available, all three of these equations are needed. The empirical determination of the bulk similarity correction functions is generally difficult, as it involves measuring the fluxes and the profiles in the whole ABL. However, the numerical simulation of ABL flows is becoming more operational and could assist greatly in the task by relating prescribed surface fluxes to concentration profiles in the convective ABL.

3.2. Rossby Number Similarity Theory

Rossby number similarity theory, which relates surface fluxes to external forces, closely parallels the extended Monin-Obukhov theory. It is tailored to large-scale modeling efforts, such as general circulation models [*Stull*, 1988], and is based upon five parameters: height above the surface (z), surface heat flux Q, friction velocity u_*, buoyancy parameter g/θ, and the Coriolis parameter f, [*Sorbjan*, 1989] [after *Kazanskii and Monin*, 1961]. Some effort has been put into using a Coriolis-based scaling length $L_E(= ku_*/f)$, known as the Ekman layer height. However, as *Sorbjan* [1989] points out, the use of f in defining a length scale can give erroneous results at low latitudes and becomes meaningless at the equator. The height of the capping inversion is believed to be a better length scale for the mixed layer [*Deardorff*, 1972]. For Rossby scaling, the profiles in the mixed layer must be matched to those in the surface layer. The equations

are similar to those of the extended Monin-Obukhov scaling.

3.3. ABL Budget Method

Another popular approach is the use of the so-called budget method, which is based on the premise that change over a time period in the amount of a scalar stored in the ABL is due to fluxes across the bottom and top boundaries of the ABL over that same time period. The entrainment flux across the top of the ABL is usually parameterized as a fixed fraction of the surface flux [*Tennekes*, 1973]. Therefore given concentration profiles at two points in time, one can "solve" for the upwind surface flux of that scalar. This approach has met considerable difficulty when applied to field measurements made with radiosondes [e.g., *Kustas and Brutsaert*, 1987]. Perhaps some improved insights can be gained from aircraft profiling methods [*Grossman*, 1991, 1992; *Betts et al.*, 1990, 1992; *Betts*, 1992; *MacPherson et al.*, 1992] and strengthening further the theory of inversion flux dynamics and entrainment parameterization [*Tennekes*, 1973; *Stull*, 1976; *Artaz and André*, 1980; *Brutsaert*, 1987].

4. LARGE EDDY SIMULATION

The flows of the ABL are governed by the Navier-Stokes equations, continuity equations, and scalar transport equations. These equations have eluded general solutions despite the great efforts of the past century. Yet while simple statistical bounds such as those described above have been developed for homogeneous flow situations, we remain unable to predict statistics for the typical flows found at larger scales over complex terrain. With mathematical solutions beyond reach, one must attempt to gain insights from observing the flow and making measurements of the dynamics and interactions. As was mentioned earlier, laboratory experiments have not met the challenge for ABL flows, as they are unable to capture the scale and complexity of the ABL. Field experiments, on the other hand, have advanced greatly our understanding of the dynamics, and they continue to do so. Nonetheless, physical constraints typically limit our ability to collect data at the space and time scales necessary to support closure model development and verification, and simplifications such as *Taylor*'s [1938] hypothesis of frozen turbulence must be introduced to bend the data to "fit" our needs. A promising tool that may substantially improve this situation is the numerical simulation of ABL flows.

4.1. Overview of the Approach

Numerical simulation of turbulence is divided into two basic classes: (1) direct numerical simulation (DNS), where all scales of the flow are resolved, from the largest energy-producing eddies down to the smallest energy-dissipating eddies, and (2) large eddy simulation (LES), where a range of scales is resolved, from the largest eddies down to an arbitrary cutoff point below which the dynamics are modeled. Resolving the flow implies that the equations of motion are integrated over a discrete mesh in time and space, as with finite difference modeling (FDM), or alternatively, they are transformed into the frequency domain and handled with spectral methods.

The ABL motions are described under the assumption of incompressible flow by the continuity equation,

$$\partial u_\alpha / \partial x_\alpha = 0 \tag{15}$$

and the equations for the conservation of momentum under the Boussinesq approximation,

$$\frac{\partial u_\alpha}{\partial t} + u_\beta \frac{\partial u_\alpha}{\partial x_\beta} = -\frac{\partial P}{\partial x_\alpha} + \nu \frac{\partial^2 u_\alpha}{\partial x_\beta \partial x_\beta} + \delta_{\alpha 3} \frac{T'}{\langle T \rangle} g \tag{16}$$

$$\alpha = 1, 2, 3$$

where u_α is the velocity in the x_α direction, P is the dynamic pressure, ν is the kinematic molecular viscosity, δ is the Kronecker delta, T' is the fluctuation of air temperature from the mean value $\langle T \rangle$, g is the acceleration of gravity, and summation is implied on any term with repeated subscripts. Note that the Coriolis term has been omitted here; it may be included or omitted in practice, depending on its relative effect on the motions. The transport of scalars, such as humidity, is represented by

$$\frac{\partial S}{\partial t} + u_\beta \frac{\partial S}{\partial x_\beta} = \nu_S \frac{\partial^2 S}{\partial x_\beta \partial x_\beta} \tag{17}$$

where S represents the scalar of interest and ν_S is the molecular diffusivity of the scalar in air.

The direct numerical simulation of ABL dynamics would require the solution of these equations (15)–(17) over a grid capable of resolving the dissipation scale of motion. Simple order of magnitude dimensional arguments suggest that this would require resolving $R^{9/4}$ degrees of freedom, where R is the Reynolds number [*McComb*, 1990]. As R can be of the order of 10^8 in the ABL, this is equivalent to a requirement of approximately 10^{18} nodes (or modes if using spectral methods). Present computing resources limit the size of practical applications to about 10^6 degrees of freedom, putting far out of reach the successful resolution of the dissipation scale within a model of the ABL. Thus our numerical modeling efforts, and accordingly our discussion here, are limited to partial resolution of the turbulence through LES. A fundamental tenet of LES is that the large scales of motion are the most dependent upon the gross flow characteristics. These structures are resolved in the LES, while the eddies smaller than some scale in the inertial subrange are modeled in terms of the resolved scales. This is a natural ap-

proach, for while the inertial subrange eddies receive their energy from the larger scales, they are also rendered statistically independent of the large-scale motion and any anisotropy that it may possess through the cascading process [e.g., *Batchelor*, 1953].

To account for this incomplete resolution, the equations of motion and transport must be modified. This is particularly important for the momentum equations, for if the dissipation scales are not resolved or otherwise accounted for, the cascading energy will accumulate in the resolved range rather than continuing downscale and ultimately being converted from mechanical to thermal energy [e.g., *Leonard*, 1974]. The velocity and scalar fields are filtered to separate explicitly the resolved from the unresolved parts. We represent a filtered flow field in a general sense by convolving a filter G over the flow field A of interest

$$\bar{A}(\mathbf{x}, t) = \int G(\mathbf{x} - \mathbf{x}')A(\mathbf{x}', t)\, d\mathbf{x}' \qquad (18)$$

where A represents u_1, u_2, u_3, or some scalar S. The actual fields can be represented by two parts: $\bar{A}$ for the resolved part and A' for the subfilter part. Applying the filter (18) to the governing equations (15)–(17) yields equations for the resolved scales which contain certain terms involving the unresolved scales A' (from the nonlinear convective term); the equations are handled numerically with the unresolved scales parameterized by a subfilter model (typically based on *Smagorinsky*'s [1963] pioneering work). The relative merit of the various filters G and subfilter models is a topic of discussion in the literature and is beyond the scope of this review. However, we should point out that many studies have reported an insensitivity of LES results to the choice of subfilter model.

As with all partial differential equations, we must specify initial and boundary conditions. The horizontal directions are typically (but not necessarily) treated with periodic boundary conditions. This is employed explicitly in finite difference LES by "wrapping" the differencing stencil from one boundary around to the other (one may visualize identical flow domains set end to end). With Fourier-based spectral methods the periodic boundary conditions are implicit to the underlying basis functions, which, by definition, are periodic. The top boundary is usually positioned well above the height of the ABL, and the capping inversion develops through the simulation and serves to keep the flow of interest well isolated from the top boundary. Therefore the simulation of ABL dynamics is relatively insensitive to the top boundary conditions, which usually involve some sort of "no-stress" lid, implying a zero vertical gradient of the longitudinal velocity at the top of the domain; similar physical arguments are used for the scalars. The bottom boundary, however, is considerably more problematic. This is because as we near the land's surface an increasingly large amount of the flux is contained in the small unresolved scales and must therefore be handled by the subfilter model. The present state of the science involves the use of relationships such as those based on Monin-Obukhov similarity theory to relate the flow quantities near the boundary to the surface fluxes across the boundary. Initial conditions are selected to be somewhat random and to satisfy (15); the integration must be carried out until the memory of the initial conditions is lost.

The interested reader should see *Rogallo and Moin* [1984] for a review of the numerical treatment of the filtered equations and *Ferziger* [1993] for an introduction to the sub-filter models. For further study, *Wendt*'s [1992] book is an accessible introduction to computational fluid dynamics (CFD) in general. Here, however, we will focus on the applications of LES to atmospheric boundary layer flows, with particular attention to its prospects for evaporation models.

We divide the literature into studies of the convective regime, the neutral and stable regimes, and studies which specifically address flow over complex terrain.

4.2. Convective Regime

Since our focus is evaporation, which occurs mainly during daylight hours when the net radiation to the Earth's surface is positive and sensible and latent heat are buoyantly transported up from the surface, we are concerned most with the convective regime of the ABL. The turbulence structure of the convective boundary layer is marked by large coherent eddies that are of a size equivalent to the depth of the ABL [*Garratt*, 1992]. We therefore have both the motivation and the justification for studying the convective regime with LES.

Deardorff [1970a, b, 1972], using a three-dimensional finite difference model, was the first to study ABL flows with LES. His simulations gave added support to the free convection theory that flow variables become independent of u_* under unstable stratification. The velocity fluctuations at heights above $-L$ (the Obukhov length) were shown to scale with w_*, the convective velocity. Furthermore, he showed that for even slightly unstable stratification the convection and turbulence extends up to the inversion base, suggesting that this height (z_i) is the most important scaling length and that $-z_i/L$ describes best the degree of instability. He also examined the shape of the eddies, which provided insight into the profiles of mean quantities, and evaluated the effect of stability on the vertical travel time of particles released near the land surface [*Deardorff*, 1972].

Moeng [1984] drew on Deardorff's work and constructed a mixed pseudospectral–finite difference LES. She used this to simulate convective flow in the ABL and compared the simulation results to experimentally derived data with reasonable success. *Wyngaard and Brost* [1984] used a finite-difference-based

LES, and *Moeng and Wyngaard* [1984] used Moeng's LES to study the entrainment of scalars into the convective boundary layer and developed expressions for the eddy diffusivities of scalars for top-down and bottom-up transport. *Holtslag and Moeng* [1991] used the LES results of *Moeng and Wyngaard* [1989] to derive an improved countergradient term for bottom-up convective transfer and expressions for the eddy diffusivities. *Holtslag and Moeng* [1991] argued that the ratio of entrainment flux to surface flux is an important factor in defining the eddy diffusivities. *Moeng and Wyngaard* [1984] used LES to study vertical profiles of the variance of a scalar being transported from the land surface. This is relevant to surface fluxes in that under free convection conditions the scalar variance in the surface layer is directly related to the surface flux of the scalar [e.g., *Albertson et al.*, 1995]. Moeng and Wyngaard report that the LES-produced scalar variance agrees with experimental data in the mixed layer but underpredicts the variance near the surface. They attribute this to the smaller scales being most active near the surface, causing much of the near-surface activity to occur in the subgrid range of motions. This is a weakness of LES and a focus of present improvement efforts [*Mason*, 1994].

Hechtel et al. [1990] used Moeng's LES to study the effect of a nonhomogeneous temperature at the surface boundary on the first and second moments of the flow field in the mixed layer. They compared the case of a nonhomogeneous boundary with the homogeneous case and found no noticeable effect. *Hadfield et al.* [1991, 1992] found notable effects on the flow characteristics in the convective ABL from surface heat flux variations. They found persistent circulations with updrafts over the high flux areas and downdrafts over the low-flux areas. They also found stronger turbulence over the heat flux maxima. A mean horizontal wind was found to diminish the circulation and transport it downstream. Much more work is needed on this topic before conclusions can be drawn safely on the effects of heterogeneous surface conditions on the structure of the ABL.

Sykes et al. [1993] used LES to study the structure of the surface layer. In particular, they addressed the instantaneous friction velocity u_* resulting from large convective structures; the probability density function was examined and found to approach Gaussian and to be insensitive to surface roughness length. Their simulations depicted variations in the surface layer depth with surface roughness length.

Schumann [1989] used a finite difference LES to study the turbulent transport of reactive and nonreactive species in the convective ABL and found both the bottom-up and top-down diffusivities to depend on reaction rates and buoyancy. For the case without reaction, the bottom-up diffusivity was found to be twice as large as the top-down diffusivity because of buoyancy effects, as was also noted by others. These results may be used to explore the conditions under which certain simple turbulence models, such as K theory, may be employed. There is a body of literature emerging on the use of LES to study the dispersion of passive and reactive scalars in the ABL [e.g., *van Haren and Nieuwstadt*, 1989, 1990; *Henn and Sykes*, 1992; *Mason*, 1992; *Nieuwstadt*, 1992a, b; *Sykes et al.*, 1992; *Sykes and Henn*, 1992]. These works have potential implications for modeling the transport of water vapor as well as pollutants and trace gases from the Earth's surface.

Schmidt and Schumann [1989] used Schumann's LES to study coherent structures in the unstable ABL. As large coherent convective structures are important flux mechanisms, their study may have direct implications for our understanding of the surface flux processes and the balance of energy at the Earth's surface. Schmidt and Schumann's results revealed that small-scale plumes that are remote from the large-scale convective plumes decay while rising through downdrafts rather than merging together. However, in the neighborhood of large thermals the smaller ones were sucked into the wake. The updrafts and downdrafts together formed a spokelike polygonal geometry, much as with Rayleigh-Benard convection, yet less regular. They sought corroborative evidence from published field data, but their efforts were less than successful. They attributed this to insufficient spatial sampling in the field and, in part, to the potential ease with which these patterns may be broken over inhomogeneous surfaces. Their results show entrainment flux at the inversion occurring through long wisps that are as long as the boundary layer is deep. These results may supplement experimental results and advance our understanding of entrainment into the ABL.

Mason [1989] has also used LES to study the convective boundary layer and investigate the effect of the mesh resolution, the domain size, and the subfilter model on the simulation results. The entrainment at the capping inversion displayed a distinct insensitivity to all three of these model characteristics. Mason reported a polygonal geometry of updrafts similar to that of *Schmidt and Schumann* [1989]. The downward entrainment of heat into the convective ABL at the inversion was resolved well by Mason's simulations, suggesting that this important process may be studied appropriately by LES. He attributes the present success, in part, to an enhanced vertical mesh resolution near the inversion and suggests that future simulations with resolutions of $\sim 128^3$ grid points hold promise for accuracy.

4.3. Neutral and Stable Regimes

While perhaps not as directly important to the study of evaporation as the convective case, neutral and stable flows do play important roles in our understanding of the dynamics of the ABL and in studying the basic form of similarity theory. It is important to note

that these flow regimes are typically dominated by structures considerably smaller than those dominating the convective flows in the ABL. Nonetheless, stable and neutral ABL flows have been studied with LES; however, the resolution of the LES can become critical.

Mason and Thomson [1987] used LES to study the neutral regime, where mechanical production of turbulence dominates over buoyant production and the size of the dominant structures scales with the height above the surface. They investigated the effect of the domain size and resolution on the LES performance with respect to roll vortices and near-surface shear instabilities. The roll vortices require a large domain, and the near-surface shearing requires a fine resolution: two competing objectives for fixed computational capabilities. Although they found that an intermediate domain scale gives the best combination of results, it was nonetheless judged to be deficient.

Mason and Derbyshire [1990] used LES to study the stable nocturnal ABL. While this topic may not be critical for evaporation research, it does have interesting applications, such as fog and pollutant transport.

4.4. Complex Terrain

LES has been used to study the effect of a wavy land surface on turbulent convection in the boundary layer [e.g., *Walko et al.*, 1992; *Schumann*, 1993; *Dornbrack and Schumann*, 1993]. *Schumann* [1993] concluded that terrain-induced coherent structures are produced only when the amplitude of the terrain undulation is large with respect to the depth of the boundary layer. He also showed the wavy terrain to have a minimal effect on the length scales for vertical velocity and vertical velocity variance, a statistic known to be important to scalar transport from the land surface [e.g., *Katul et al.*, 1994a]. *Walko et al.* [1992] also studied the effect of hilly terrain on the convective ABL (200-m hills in 1-km-deep boundary layer), but they found noticeable effects on certain flow measures. Interestingly, Walko et al. found the horizontally averaged statistics of flow over hilly terrain to be similar to those obtained over flat terrain; however, they found significant effects in the spectra and also found pronounced amounts of subgrid turbulent kinetic energy and vertical heat flux above the higher terrain. These results, when considered along with those from field investigations over similar terrain [e.g., *Kustas and Brutsaert*, 1986], may lend insight into the effect of nonideal terrain on simple turbulence models that are based on homogeneity assumptions. The turbulent structure of upslope boundary layers is also being investigated with LES [e.g., *Schumann*, 1990].

In a unique study, *Shaw and Schumann* [1992] simulated the atmospheric surface layer above and within a forest. Their flow domain extended only three forest heights in the vertical and therefore did not encompass the entire depth of the ABL. This limited vertical extent is charged with causing some departure of the simulation results from field experimental evidence. However, they did capture some features noted in field data. Perhaps most important about this study is that it opened to LES modeling of the ABL over forested landscape. Extensions of this work using larger flow domains could leverage the results of field experience over complex forest terrain [e.g., *Brutsaert and Parlange*, 1992; *Parlange and Brutsaert*, 1993] toward an improved understanding of regional surface fluxes.

5. LARGE-SCALE ATMOSPHERIC MEASUREMENT

5.1. Introduction

Our ability to understand and formulate the theoretical basis for the physics of ABL transport is determined largely by our ability to make measurements. A great leap in our understanding of atmospheric turbulence occurred around 1970 with the introduction of practical instruments capable of making fast measurements of wind, temperature and humidity. While great progress has been made using these instruments, they are not capable of defining the details of the three-dimensional flow field as it evolves in time.

Sensors used to make measurements in the atmospheric boundary layer fall generally into two categories: point sensors intended for use on the ground, towers, or balloons; and remote sensors, which can sense atmospheric properties over some area or volume. Point sensors include such devices as cup, vane, and sonic anemometers; thermistors, thermocouples, and resistance thermometers; dew point, ultraviolet absorption, and capacitance hygrometers; and net radiometers, soil heat flux plates, and lysimeters. An excellent review of these devices and their operating principles, capabilities, and limitations is given by *Kaimal and Finnigan* [1994].

Remote sensors, such as radar, sodar, lidar, and aircraft-based instruments, measure atmospheric properties over large areas or volumes. These types of sensors are being used more often in atmospheric boundary layer measurements. They are capable of making time-resolved vertical profiles or multidimensional measurements of atmospheric properties, which are useful in examining the evolution of large-scale features such as boundary layer depth, layering, and flow fields. Techniques have been developed for many of the instruments to measure the fluxes of heat, momentum, or water vapor over some area. These instruments share a number of shortcomings, not the least of which are cost, complexity, and portability. Individual instruments suffer from such limitations as accuracy, minimum or maximum range, and range resolution. The theoretical bases of these devices and the data interpretation algorithms are not as well developed as those for surface point sensors. Moreover, the analy-

sis of the vast amounts of data generated by these devices is generally complex and time intensive. But, of course, when applied properly, the information provided by these sensors can be extremely useful to support the visualization of flow and transport through space.

5.2. Sound Detection and Ranging (Sodar)

Sodars send out a pulse of sound as a probe and analyze the returning echoes in a manner similar to sonar. Sound will echo from variations in density of the atmosphere caused by temperature and velocity fluctuations. A Doppler sodar measures the component of the wind velocity along the line of sight from the difference in frequencies between the return echo and the transmitted pulse. When this measurement is made in several directions, the three-dimensional wind field can be established. This can be done using multiple transmitter-receivers or with a phased transmitter array. Details on the method are given by *Little* [1969] or *Beran and Clifford* [1972]. In addition to the wind velocity, the range-resolved temperature and velocity structure parameters, C_t and C_v, can be determined. From this information, the sensible heat flux, momentum flux, eddy viscosity, and atmospheric stability can be calculated [*Dahlquist*, 1993; *Quintarelli*, 1993; *Coulter and Wesely*, 1980; *Beyrich and Kotroni*, 1993]. Sodars generally do not scan, and, therefore they provide only a vertical profile of the atmosphere as a function of time. However, they are sensitive to the amount of background noise and are therefore range-limited in noisy environments such as cities. Despite this limitation, sodars have been used successfully in a large number of experiments in cities [*Gera and Singal*, 1990; *Pekour and Kallistratova*, 1993; *Singal*, 1993], in pollution monitoring [*Asimakopoulos*, 1991], and at remote sites [*Gera and Weill*, 1990; *Cheung*, 1991; *Cheung and Little*, 1990; *Argentini et al.*, 1992]. Comparisons between sodars and conventional instruments have been accomplished on many occasions with favorable results [*Kaimal and Finnigan*, 1994; *Melas*, 1990; *Parlange and Brutsaert*, 1990; *Thomas and Vogt*, 1993a, b; *Beyrich*, 1992]. Because of the sharp change in temperature between atmospheric layers, the sodar is particularly well suited to the examination of these layers and the study of entrainment at the top of the boundary layer [*Frisch and Clifford*, 1974; *Beyrich and Weill*, 1993]. This technology is best developed of all the remote sensors [*Sorbjan et al.*, 1991; *Melas*, 1993] and is commercially available, reliable, and relatively inexpensive in comparison with most remote sensors. Furthermore, it is capable of operating with a minimum of operator intervention.

5.3. Radio Detection and Ranging (Radar)

The use of radar in atmospheric research grew from the study of "weather clutter," which confused operators in the early days of its use as an aircraft locator. Radars use a pulse (or pulses) of radio frequency energy to probe the atmosphere. These radio waves scatter from small density variations in the air, whose size is of the order of the radar's wavelength (from a few to tens of centimeters). The density variations are caused by pressure, temperature, or humidity variations indicative of turbulent mixing or layering. Changes in density change the index of refraction of the air in those locations. The sensitivity to changes in air temperature makes radars useful in the study of the capping of the boundary layer [e.g., *Frisch and Clifford*, 1974]. Through the use of the Doppler effect, in which the returning wave is shifted in frequency by an amount determined by the velocity of the structure, wind speeds can be determined along that line of sight. By scanning at several angles (through multiple transmitters, or through phased array methods), a map of the three-dimensional wind field can be constructed [*Banta et al.*, 1993; *Ralph et al.*, 1993; *Fukao et al.*, 1982;, *Warnock et al.*, 1978; *Eilts*, 1987]. Techniques for using this type of information to determine fluxes of heat and momentum in the boundary layer are given by *Gossard et al.* [1982] and *Angevine et al.* [1993a]. *Wilson* [1970] has described an analysis technique that can be used to estimate the velocity variances and covariances by measuring the spectral purity of the Doppler-shifted return.

"Chaff," tiny aluminized filaments cut to a length of half the radar wavelength, has been used to increase the signal return for radars. These filaments can be easily dispersed and will travel with the wind for a period of several hours before settling out. The large increase in signal returned has the benefit that the averaging time is greatly reduced and the accuracy and range resolution is increased. This enables fast, accurate, high-resolution measurements to be made throughout the depth of the boundary layer. An example of the study of diffusion in the atmosphere using chaff in the Convective Diffusion Observed by Remote Sensors (CONDORS) experiment is given by *Briggs* [1993]. Examples of natural "chaff" are rain, snow, and clouds. In an interesting use of the radar with this natural signal enhancement, *Russchenberg* [1993] measured the size distribution of rain droplets. The weather radar shown on the television is another example of an enhanced return from clouds.

Radio acoustic sounding (RASS) is a combination of Doppler radar and sodar techniques. The radar is used to track the progress of a sound pulse as it propagates through the atmosphere. Variations in the speed of that pulse (which travels at the local speed of sound at each position) are proportional to the square root of the virtual temperature [*May et al.*, 1990]. This method is capable of fine detail [*Currier et al.*, 1988] but is limited by strong winds or turbulence, which transport and distort the sound wave so that the sound and radar wave fronts are no longer aligned. Thus while the range resolution is often good, the maximum

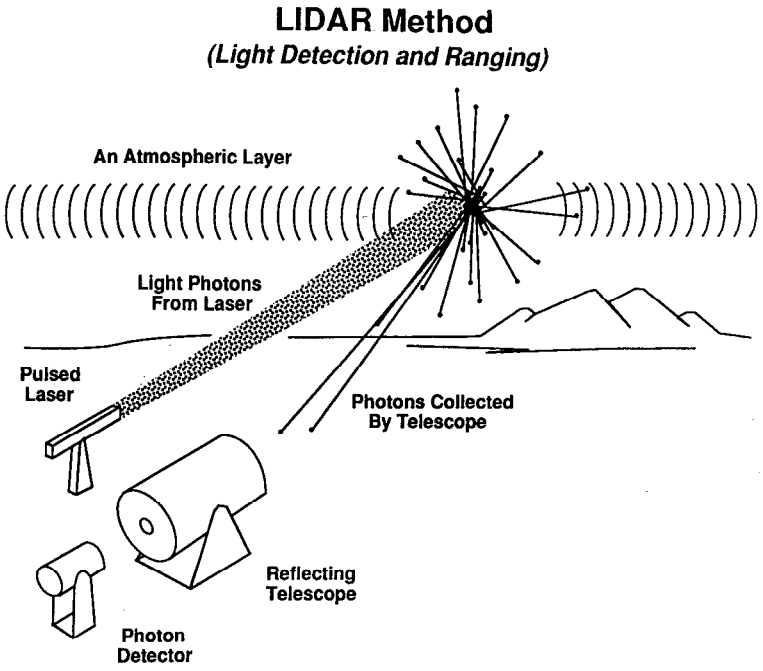

Figure 4. A schematic diagram of a lidar system. Lidars are typical of active remote sensors in that they project a beam into the atmosphere (in this case a beam of laser light) and sample the returning signal to determine the properties of the atmosphere in multiple dimensions. While different sensors may use different components (an antenna for a radar instead of a telescope), the basic functional elements are similar.

range is limited to less than a kilometer. A comparison of RASS with aircraft measurements was accomplished by *Angevine et al.* [1993b].

Depending on the details of each system, radars are capable of the longest ranges of any of the remote sensors (approaching 100 km) and provide competitive range resolutions (as low as 1.5 m). As with all of the systems examined here, they are expensive and complex. They also require trained operators and may have safety issues associated with high transmitted power densities.

5.4. Light Detection and Ranging (Lidar)

Lidars, in which visible or near-visible light is used as the probe, are available in several varieties. They are all similar in that they use a pulsed laser beam as a source of the light, and they rely on some type of interaction to affect the outgoing light and scatter some of the resulting light back to be collected by a telescope. The detector(s) at the back of the telescope converts the collected light to an electrical signal, which is then sampled and stored in a computer [*Measures*, 1984, 1988] (see Figure 4). Data analysis methods for determining atmospheric properties from lidar measurements are not as well developed as those for the other remote sensors; however, progress is being made [*Eichinger et al.*, 1993b; *Eloranta and Forest*, 1992; *Eloranta and Schols*, 1990; also Parlange et al., submitted manuscript, 1995]. Despite the infancy of data analysis algorithms, lidars have been particularly useful in verifying various atmospheric and plume dispersion models [*Beniston et al.*, 1990; *Boers et al.*, 1991; *Bennett et al.*, 1992; *Jorgensen and Mikkelsen*, 1993; *Briggs*, 1993].

Elastic lidars rely on elastic photon interactions where the returning light has the same wavelength as the laser transmission. This type of interaction with molecules and particulates in the atmosphere has a large cross section (i.e., the ratio of the amount of light returning to the amount of light transmitted is large). Elastic lidars are generally the smallest and fastest scanning of the various lidars. Accordingly, they are ideally suited to tracking the motion of structures in real time or mapping structure shape over a large volume. In general, since these devices are sensitive to large (0.5 to 10 μm) atmospheric particulates, such as typical pollutants, they are often used for the study of pollution [*Hashmonay et al.*, 1991; *Asimakopoulos*, 1991] or plume dynamics. Plates 1 and 2 are examples of the vertical distribution of aerosols over Mexico City and Barcelona. In these figures, sources of pollution such as roads are readily identified by the high density near the surface (the highest densities being the color red). A traditional problem with elastic lidars is that a unique inversion of the signal to obtain aerosol concentrations is not possible. While various solutions have been proposed [*Ferguson and Stephens*, 1983; *Klett*, 1981, 1985; *Mulders*, 1984], they all contain assumptions that are sufficiently restrictive to limit their usefulness. An exception is the high spectral resolution elastic lidars pioneered by Eloranta [*Grund and Eloranta*, 1990, 1991], which can separate the molecular and aerosol returns and generate a unique solution to obtain the optical properties of the particulates. The sensitivity of elastic lidars to small changes in aerosol density makes them ideal for the determination of wind velocity [*Hooper and Eloranta*, 1986; *Eloranta and Schols*, 1990; *Schols and Eloranta*, 1990; *Barber and Weinman*, 1990; *Kolev et al.*, 1988; *Sasano et al.*, 1986; *Sroga and Eloranta*, 1980; *Kunkel et al.*,

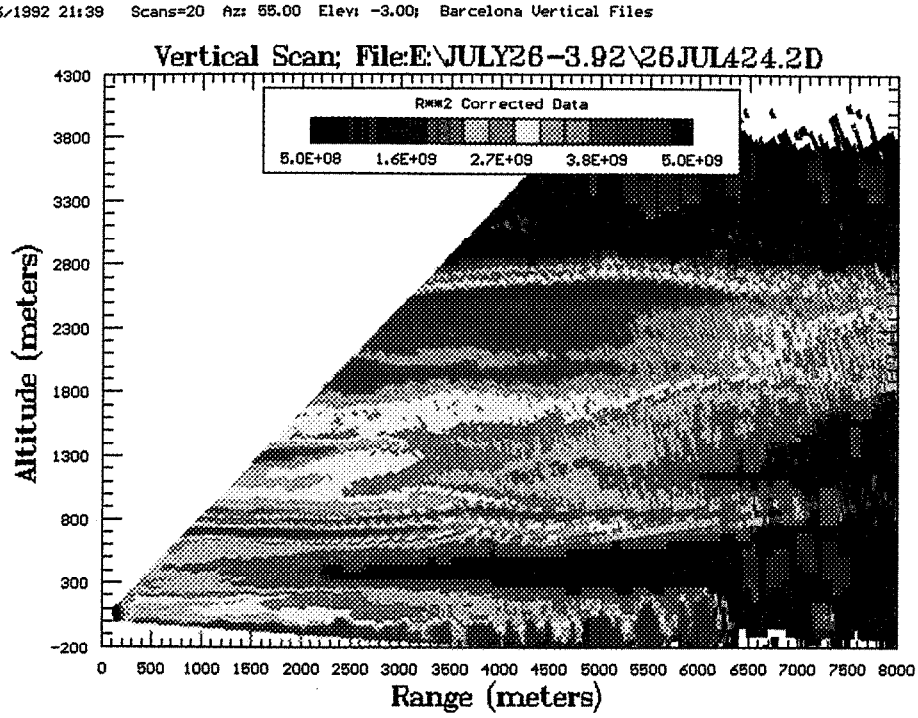

Plate 1. Vertical scan over the city of Barcelona, Spain, taken with the Los Alamos lidar. Large structures with high aerosol concentrations are visible as large red plumes near the ground. Higher up in the atmosphere, other layers with high concentration can be found. Plots such as this can be used to study the origin and transport of pollution in the city, the transport of pollution through the city from outside sources, and the effects of remediation efforts. With respect to regional evaporation, much can be learned about the structure and the time evolution of the ABL.

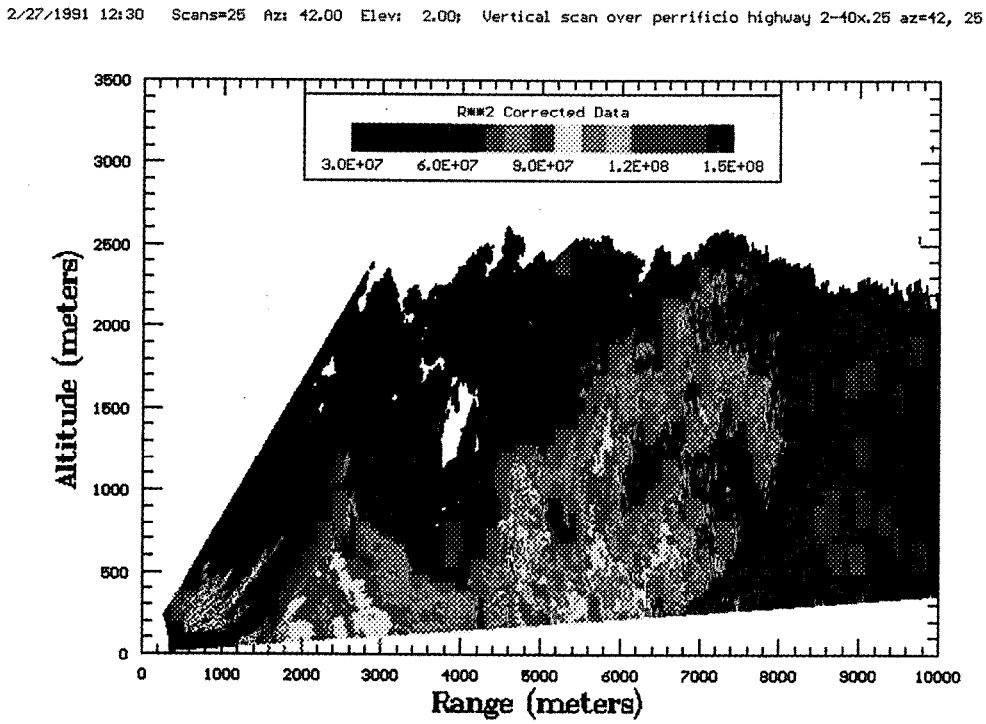

Plate 2. Example of the vertical distribution of aerosols over Mexico City. In these figures, sources of pollution such as roads are readily identified by the high density near the surface (the highest densities being the color red). Notice the relatively clean free-atmosphere air (white) which has been entrained into the ABL. These measurements allow us to improve our understanding of the physical mechanisms acting throughout the ABL.

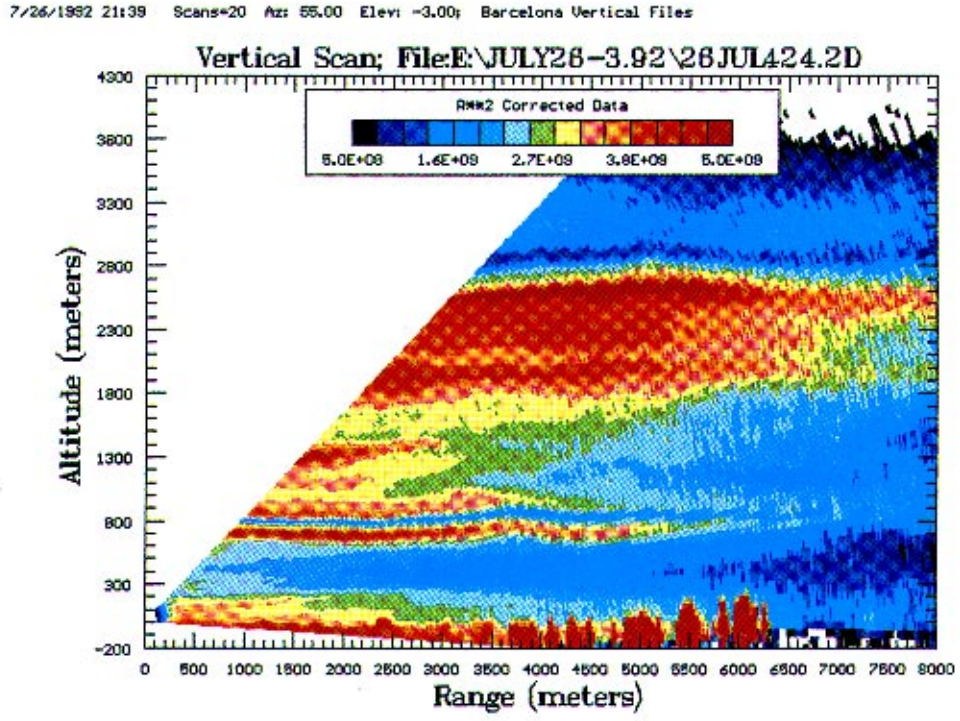

Plate 1. Vertical scan over the city of Barcelona, Spain, taken with the Los Alamos lidar. Large structures with high aerosol concentrations are visible as large red plumes near the ground. Higher up in the atmosphere, other layers with high concentration can be found. Plots such as this can be used to study the origin and transport of pollution in the city, the transport of pollution through the city from outside sources, and the effects of remediation efforts. With respect to regional evaporation, much can be learned about the structure and the time evolution of the ABL.

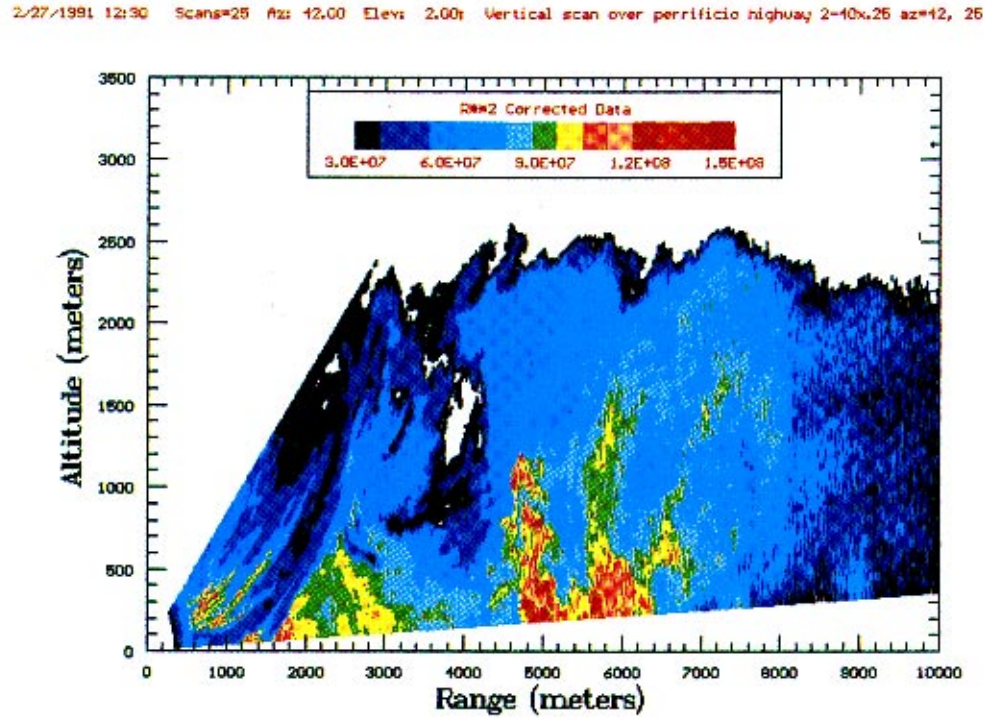

Plate 2. Example of the vertical distribution of aerosols over Mexico City. In these figures, sources of pollution such as roads are readily identified by the high density near the surface (the highest densities being the color red). Notice the relatively clean free-atmosphere air (white) which has been entrained into the ABL. These measurements allow us to improve our understanding of the physical mechanisms acting throughout the ABL.

TABLE 2. Molecules Detected With Lidar in the Infrared

Molecule	*Wavenumber*	*Reference*
Nitrous oxide (NO)	1881.098	*Killinger and Menyuk* [1981], *Menyuk et al.* [1980], *Hinkley et al.* [1976]
	1900.1	
Carbon monoxide (CO)	2154.604	*Killinger et al.* [1980]
Ethylene (C_2H_4)	949.48	*Killinger and Menyuk* [1981], *Mayer et al.* [1978]
Freon 11 (CCl_3F)	1084.0	*Mayer et al.* [1978]
Freon 12 (CCl_2F_2)	932.9	*Mayer et al.* [1978]
Freon 113 ($C_2Cl_3F_3$)	1041.2	*Hinkley et al.* [1976]
Ozone (O_3)	1052.2	*Mayer et al.* [1978], *Grant* [1986], *McDermid* [1993]
Sulfur dioxide (SO_2)	1139.60	*Baumgartner and Byer* [1978], *Hinkley et al.* [1976]
	1108.2	
Benzene (C_6H_6)	1039.4	*Mayer et al.* [1978]
Chloroprene (C_4H_5Cl)	974.6	*Mayer et al.* [1978]
Sulfur hexafluoride (SF_6)	947.8	*Englisch and Wiesemann* [1978], *Uthe* [1986]
Trichloroethylene ($C_2H_4Cl_3$)	944.2	*Mayer et al.* [1978]
Hydrazine (N_2H_4)	942.3	*Menyuk et al.* [1982], *Grant* [1986]
	924.973	
Ammonia (NH_3)	1084.6	*Hinkley et al.* [1976], *Grant* [1986], *Mayer et al.* [1978]
	980.913	
	967.8	
Water vapor (H_2O)	974.621	*Grant* [1986]
Perchloroethylene (C_2Cl_4)	944.2	*Hinkley et al.* [1976]

1980] and the study of entrainment at the top of the boundary layer [*Glaser et al.*, 1993; *Hooper and Eloranta*, 1986].

Doppler lidars use the Doppler shift from the scattering of particulates to measure the wind velocity. A pulse of light is emitted by the laser, which has a narrow wavelength band. The returning light is Doppler shifted in wavelength because of the relative velocity of the particles. The shift is measured by mixing the returning light with light of the original wavelength and measuring the beat frequency that results. From this frequency the component of the wind velocity along the line of sight can be determined at various ranges. A three-dimensional wind field is determined by scanning the lidar in some predetermined pattern (usually an inverted cone) and assuming the flow field to be uniform inside the scanned area [*Garnier and Chanin*, 1992]. Various turbulence parameters and the momentum flux have been determined by *Galchen et al.* [1992]. A number of comparisons between conventional instruments and Doppler lidar have been performed [*Kormakov et al.*, 1993].

Raman lidars use the Raman effect to identify specific molecules. Because this effect is weak, it is appropriate only when the molecular concentration is large or when a long averaging time can be tolerated. By comparing the Raman-shifted returning light from the molecule of interest to that from atmospheric nitrogen, the absolute concentration of that molecule can be determined [*Melfi et al.*, 1969; *Cooney*, 1970]. While Raman lidars can be used to detect nearly any molecule (e.g., by *Bilbe et al.* [1990] to detect natural gas), these systems are most often used to measure vertical profiles of water vapor concentration over averaging times of the order of 5 min with maximum range of 4 to 10 km [*Vaughn et al.*, 1988; *Melfi et al.*, 1989; *Whiteman et al.*, 1992]. They can also be used to measure the water vapor concentrations vertically and horizontally in a scanning mode with range limited to about 700 m, as well as the vertical flux of water vapor [*Eichinger et al.* 1993a, 1994]. Raman lidars are also useful in that the nitrogen Raman signal can be used to invert the signal to obtain a unique set of aerosol optical properties [*Ansmann et al.*, 1991, 1992, 1993; *Mitev et al.*, 1992]. This type of lidar can also measure atmospheric temperatures and pressures [*Ivanova*, 1993; *Nedeljkovic et al.*, 1993; *Arshinov et al.*, 1983].

Differential absorption lidar (DIAL) is used to sense specific molecules. With this method, two wavelengths are chosen which have similar propagation properties, but one of the wavelengths is strongly absorbed by the molecule of interest and the other is not; thus the difference between the two returning signals is indicative of the absolute concentration of the species of interest. This methodology can be used to map the concentration of this species in several dimensions. This has been done for a great number of molecules. While beyond the scope of the present paper, an incomplete list of some molecules of environmental interest that can be measured by this instrument in both the infrared and ultraviolet–visible portions of the spectrum is included in Tables 2 and 3 to show the breadth of capability of this instrument [*Gall et al.*, 1991]. These molecules can be mapped with a range resolution that depends on the concentration of the molecule, the strength of the interaction, and the averaging time of the lidar. An excellent review of the

TABLE 3. Molecules Detected With Lidar in the UV and Visible

Molecule	*Wavelength, nm*	*Reference*
Nitrous oxide (NO_2)	448.2	*Hinkley et al.* [1976]
Water vapor (H_2O)	724.37	*Browell et al.* [1980]
Ozone (O_3)	253.6	*Hinkley et al.* [1976]
Sulfur dioxide (SO_2)	300.1	*Hinkley et al.* [1976]
Benzene (C_6H_6)	252.9	*Milton et al.* [1992]
Toluene (C_6H_5OH)	256.3	*Milton et al.* [1992]
Xylene (C_6H_6-$2CH_3$)	187	*Suto et al.* [1992]
Nitrogen monoxide (NO)	214.9	*Suto et al.* [1992]

use of Raman lidars and DIAL systems to detect water vapor is given by *Grant* [1990].

Lidars are capable of good spatial resolution (1.5 m to 15 m is typical) and intermediate range (from 3 to 12 km). They have the capability of providing a wide range of information on the atmosphere. However, the algorithms for using the information to derive parameters of interest to the atmospheric scientist are generally not well developed.

5.5. Aircraft Measurements

Instrumented aircraft are now commonly used in most large-scale experiments. The instruments used are, in principle, the same as those used on the surface and measure essentially the same parameters: the means and variances of temperature, humidity, wind velocity, upwelling and downwelling longwave and shortwave radiation, particulate sizes, and the concentration of various molecules [*Scott et al.*, 1990]. The advantage of aircraft is that they can cover a large area rapidly and do so at a number of altitudes in the boundary layer. That the aircraft is a moving platform is also a serious limitation; corrections need to be applied for the motion of the aircraft and the flow distortions inherent in the platform [*Crawford et al.*, 1993; *Grossman*, 1992; *Schuepp et al.*, 1992].

Instrumented aircraft have been used successfully in a large number of experiments [*MacPherson et al.*, 1992; *Mahrt and Ek*, 1993]. Comparisons have been made with conventional instruments and methods [*Chou*, 1993; *Lenschow et al.*, 1991; *DesJardins et al.*, 1989], as well as with lidars, sodars, and other remote sensors [*Angevine et al.*, 1993b]. The study of aircraft data has initiated interest in the source regions or footprints from which a given signal originates [*Schuepp et al.*, 1990]. Recent advances in the application of aircraft for eddy correlation and flux gradient measurements are presented by *Mann and Lenschow* [1994] and *Lenschow et al.* [1994].

An especially notable accomplishment is the installation of a DIAL system aboard an aircraft by *Browell et al.* [1980, 1983]. This system is capable of measuring water vapor and ozone and has been used in a large number of experiments around the globe at locations which are essentially inaccessible to conventional instrumentation.

5.6. Scintillometry

A scintillometer is neither a point instrument nor truly a remote sensor. It is a device that measures the amount of refraction of laser light by density fluctuations in the atmosphere over distances of several hundred meters. From these measurements the turbulence inner scale and the temperature structure parameter C_t can be determined. Through the use of multiple wavelengths and advanced analysis techniques, the velocity and humidity structure parameters C_u and C_q can also be determined [*Kohsiek*, 1988]. These parameters provide indirect measurements of the average dissipation rates of turbulent kinetic energy, temperature variance, and humidity variance. From these we may calculate the fluxes of momentum, heat, and water vapor over the distance of the measurements. A number of experiments have been conducted to verify the accuracy of the technique for flux estimation [*Coulter and Wesely*, 1980; *Hill et al.*, 1992] and to compare the various analysis methods [*Hill*, 1988].

Scintillometers are the cheapest of the instruments described here and are also the simplest to operate. They are relatively rugged and capable of running unattended. Their use is complicated by the fact that several assumptions are implicit in processing the data and that the fluxes estimated are areal averages.

6. CONCLUSIONS

An accurate description of evaporation into the atmosphere, at the scales of interest, is necessary if we are to improve our understanding of regional and global hydrology. The success or failure of any effort to measure or predict the various components of the land surface hydrologic balance is naturally linked to the accuracy to which the quantification of evaporation over catchment or water basin scale areas is possible. Given the heterogeneity found at the land surface and the variable surface fluxes within the region of interest, the turbulent atmosphere plays a useful role in terms of mixing and blending the water vapor emitted from the spatially variable surface conditions. A better understanding of turbulent transfer in the atmospheric boundary layer at the appropriate scales will lead to improved parameterization of evaporation and could ultimately provide the basis for more refined techniques for the solution of practical hydrologic problems.

To understand transport at the scales of interest in hydrology, it is important to measure evaporative processes directly at those scales. Based on a number of recent large-scale field experiments, similarity formulations that were developed for local field sites have been successfully applied to ABL profile measure-

ments of wind speed, temperature, and humidity to obtain regional scale surface fluxes. Many of the field measurement tools of the past have been based upon point sensors or radiosondes to probe the ABL. Techniques for remotely sensing atmospheric properties, especially the application of lidar, provide a new opportunity to capture and understand the three-dimensional mixing processes in the boundary layer. Remote-sensing tools are opening new windows for describing the transport of scalars from the surface, the structure of the flux-carrying eddies, the entrainment at the top of the boundary layer, and the effects of complex terrain on the structure and mixing of the ABL. Computational approaches, in particular LES, also provide opportunities to visualize transport mechanisms in the ABL and provide insight into physical mechanisms. LES will become an even more productive tool as our simulations become better tailored to the ABL characteristics and as computational capabilities continue to advance. This combination of field measurements, ABL similarity modeling, and numerical simulations is providing a timely advancement of our understanding of land surface fluxes and the ABL.

ACKNOWLEDGMENTS. This work has been supported and financed, in part, by the National Science Foundation (EAR-93-04331), the California State Salinity Drainage Task Force, the Kearney Foundation; California Water Resources Center (W-182), the UC Davis Superfund grant (5 P42ES04699-07); and, the NASA Graduate Student Fellowship in Global Change Research program. The authors thank Editor James A. Smith and Editor-in-Chief Alan D. Chave for their encouragement and invitation to submit. The three anonymous referees are thanked for their constructive comments.

REFERENCES

Albertson, J. D., M. B. Parlange, G. G. Katul, C.-R. Chu, H. Stricker, and S. Tyler, Sensible heat flux from arid regions: A simple flux variance method, *Water Resour. Res.*, in press, 1995.

André, J.-C., P. Lacarrère, and L. J. Mahrt, Sur la distribution verticale de l'humidité dans une couche limite convective, *J. Rech. Atmos.*, *13*, 135–146, 1979.

André, J.-C., J.-P. Goutorbe, and A. Perrier, HAPEX-MOBILHY: A hydrologic atmospheric experiment for the study of water budget and evaporation flux at the climate scale, *Bull. Am. Meteorol. Soc.*, *67*, 138–144, 1986.

André, J.-C., et al., Evaporation over land-surfaces: First results from HAPEX-MOBILHY special observing period, *Ann. Geophys.*, *6*, 477–492, 1988.

André, J.-C., P. Bougeault, J.-F. Mahfouf, P. Mascart, J. Noilhan, and J.-P. Pinty, Impact of forest on mesoscale meteorology, *Philos. Trans. R. Soc. London B*, *324*, 407–422, 1989.

Angevine, W., S. Avery, W. Ecklund, and D. Carter, Fluxes of heat and momentum measured with a boundary layer wind profile radar radio acoustic sounding system, *J. Appl. Meteorol.*, *32*, 73–80, 1993a.

Angevine, W., S. Avery, and G. Kok, Virtual heat flux measurements from a boundary layer profile RASS compared to aircraft measurements, *J. Appl. Meteorol.*, *32*, 1901–1907, 1993b.

Anselmet, F., Y. Gagne, E. J. Hopfinger, and R. A. Antonia, High-order velocity structure functions in turbulent shear flows, *J. Fluid Mech.*, *140*, 63–89, 1984.

Ansmann, A., M. Riebesell, U. Wandinger, W. Michaelis, and C. Weitkamp, Klett forward-backward integration for model dependent determination of the aerosol extinction to backscatter ratio, GKSS-Forschungszentrum Geesthacht GmbH, Geesthacht, Germany, 1991.

Ansmann, A., U. Wandinger, M. Riebesell, C. Weitkamp, and W. Michaelis, Independent measurement of extinction and backscatter profiles in cirrus clouds by using a combined Raman elastic-backscatter lidar, *Appl. Opt.*, *31*, 7113–7131, 1992.

Ansmann, A., J. Bosenberg, G. Brogniez, and S. Elouragini, Lidar network observations of cirrus morphological and scattering properties during the International Cirrus Experiment 1989—The 18 October 1989 case study and statistical analysis, *J. Appl. Meteorol.*, *32*, 1608–1622, 1993.

Antonia, R. A., Conditional sampling in turbulence measurement, *Annu. Rev. Fluid. Mech.*, *13*, 131–156, 1981.

Argentini, S., G. Mastrantonio, G. Fiocco, and R. Ocone, Complexity of the wind field as observed by a sodar system and by automatic weather stations on the Nansen Ice Sheet, Antarctica, during summer 1988–89—2 case studies, *Tellus, Ser. B*, *44*, 422–429, 1992.

Arshinov, Y. F., S. M. Bobrovnikov, V. E. Zuev, and V. M. Mitev, Atmospheric temperature measurements using a pure rotational Raman lidar, *Appl. Opt.*, *22*, 2984–2990, 1983.

Artaz, M.-A., and J.-C. André, Similarity studies of entrainment in convective mixed layers, *Boundary Layer Meteorol.*, *19*, 51–66, 1980.

Arya, S. P. S., and J. C. Wyngaard, Effect of baroclinicity on wind profiles and the geostrophic drag laws for the convective planetary boundary layer, *J. Atmos. Sci.*, *32*, 767–778, 1975.

Asimakopoulos, D. N., Application of sodar and lidar techniques in air pollution monitoring—A report on the Eurasap-90 International Meeting, *Atmos. Environ., Part A*, *25*, 2057–2060, 1991.

Aurell, E., U. Frisch, J. Lutsko, and M. Vergassola, On the multifractal properties of the energy dissipation derived from turbulence data, *J. Fluid Mech.*, *238*, 467–486, 1992.

Avissar, R., and R. A. Pielke, A parameterization of heterogeneous land-surface for atmospheric numerical models and its impact on regional meteorology, *Mon. Weather Rev.*, *117*, 2113–2136, 1989.

Avissar, R., and M. M. Verstraete, The representation of continental surface processes in atmospheric models, *Rev. Geophys.*, *28*, 35–52, 1990.

Baldocchi, D. D., and T. P. Meyers, The effects of extreme turbulent events on the estimation of aerodynamic variables in a deciduous forest canopy, *Agric. For. Meteorol.*, *48*, 117–134, 1989.

Banta, R. M., L. D. Olivier, and D. H. Levinson, Evolution of the Monterey Bay sea-breeze layer as observed by pulsed Doppler lidar, *J. Atmos. Sci.*, *50*, 3959–3982, 1993.

Barber, T. L., and J. A. Weinman, A portable lidar boundary-layer wind profiling system, *J. Atmos. Oceanic Technol.*, *7*, 177–179, 1990.

Barros, A. P., Dynamic modeling of orographically induced precipitation, *Rev. Geophys.*, *32*, 265–284, 1994.

Batchelor, G. K., *The Theory of Homogeneous Turbulence*, 197 pp., Cambridge University Press, New York, 1953.

Baumgartner, R., and R. Byer, Remote SO_2 measurement at 4 microns with a continuously tunable source, *Opt. Lett.*, *2*, 163–165, 1978.

Beniston, M., J. Wolf, M. Benistonrebetez, and H. Kolsch, Use of lidar measurements and numerical models in air pollution research, *J. Geophys. Res.*, *95*, 9879–9894, 1990.

Bennett, M., S. Sutton, and D. Gardiner, Measurements of wind speed and plume rise with a rapid-scanning lidar, *Atmos. Environ., Part A*, *26*, 1675–1688, 1992.

Beran, D., and S. Clifford, Acoustic Doppler measurement of the total wind vector, paper presented at Second Symposium on Meteorological Observation and Instrumentation, Am. Meteorol. Soc., San Diego, Calif., 1972.

Betchov, R., and A. M. Yaglom, Comments on the theory of similarity as applied to turbulence in an unstably stratified fluid, *Izv. Acad. Sci. USSR Atmos. Oceanic Phys.*, Engl. Transl., *7*, 829–832, 1971.

Betts, A. K., FIFE atmospheric boundary layer budget methods, *J. Geophys. Res.*, *97*, 18,523–18,531, 1992.

Betts, A. K., R. L. Desjardins, J. I. MacPherson, and R. D. Kelly, Boundary layer heat and moisture budgets from FIFE, *Boundary Layer Meteorol.*, *50*, 109–137, 1990.

Betts, A. K., R. L. Desjardins, and J. I. MacPherson, Budget analysis of the boundary layer grid flights during FIFE 1987, *J. Geophys. Res.*, *97*, 18,533–18,546, 1992.

Beyrich, F., Sodar estimates of surface heat flux and mixed layer depth compared with direct measurements, *Atmos. Environ., Part A*, *26*, 2459–2461, 1992.

Beyrich, F., On the use of sodar data to estimate mixing height, *Appl. Phys. B*, *57*, 27–35, 1993.

Beyrich, F., and V. Kotroni, Estimation of surface stress over a forest from sodar measurements and its use to parameterize the stable boundary-layer height, *Boundary Layer Meteorol.*, *66*, 93–103, 1993.

Beyrich, F., and A. Weill, Some aspects of determining the stable boundary layer depth from sodar data, *Boundary Layer Meteorol.*, *63*, 97–116, 1993.

Bilbe, R., S. Bullman, and F. Swaffield, An improved Raman lidar system for the remote measurement of natural gas releases into the atmosphere, *Meas. Sci. Technol.*, *1*, 495–499, 1990.

Boers, R., S. H. Melfi, and S. P. Palm, Cold-air outbreak during gale—Lidar observations and modeling of boundary layer dynamics, *Mon. Weather Rev.*, *119*, 1132–1150, 1991.

Bolle, H. J., et al., EFEDA—European field experiment in a desertification-threatened area, *Ann. Geophys.*, *11*, 173–189, 1993.

Bouchet, R. J., Evapotranspiration réelle, évapotranspiration potentielle, et production agricole, *Ann. Agron.*, *14*, 743–824, 1963.

Bougeault, P., J. Noilhan, P. LaCarrere, and P. Mascart, An experiment with an advanced surface parameterization in a mesobeta-scale model, 1, Implementation, *Mon. Weather Rev.*, *119*, 2358–2373, 1991.

Bouttier, F., J. F. Mahfouf, and J. Noilhan, Sequential assimilation of soil moisture from atmospheric low-level parameters, 1, Sensitivity and calibration studies, *J. Appl. Meteorol.*, *32*, 1335–1351, 1993.

Briggs, G., Final results of the Condors convective diffusion experiment, *Boundary Layer Meteorol.*, *62*, 315–328, 1993.

Browell, E., A. Carter, and T. Wilkerson, An airborne water-vapor lidar system, in *Atmospheric Water Vapor*, edited by A. Deepak, T. Wilkerson, and L. Ruhnke, pp. 461–476, Academic, San Diego, Calif., 1980.

Browell, E., A. Carter, S. Shipley, R. Allen, C. Butler, M. Mayo, J. Siviter, and W. Hall, NASA Multipurpose Airborne DIAL System and measurements of ozone and aerosol profiles, *Appl. Opt.*, *22*, 522–534, 1983.

Brutsaert, W., *Evaporation Into the Atmosphere: Theory, History and Applications*, 229 pp., D. Reidel, Norwell, Mass., 1982.

Brutsaert, W., Catchment scale evaporation and the atmospheric boundary layer, *Water Resour. Res.*, *22*, suppl., 39S–45S, 1986.

Brutsaert, W., Nearly steady convection and the boundary-layer budgets of water vapor and sensible heat, *Boundary Layer Meteorol.*, *39*, 283–300, 1987.

Brutsaert, W., The formulation of evaporation from land surfaces, in *Recent Advances in the Modeling of Hydrologic Systems*, edited by D. S. Bowles and P. E. O'Connell, pp. 67–84, Kluwer Academic, Norwell, Mass., 1991.

Brutsaert, W., The unit response of groundwater outflow from a hillslope, *Water Resour. Res.*, *30*, 2759–2763, 1994.

Brutsaert, W., and W. Kustas, Evaporation and humidity profiles for neutral conditions over rugged hilly terrain, *J. Clim. Appl. Meteorol.*, *24*, 915–923, 1985.

Brutsaert, W., and J. A. Mawdsley, The applicability of planetary boundary layer theory to calculate regional evaporation, *Water Resour. Res.*, *12*, 852–858, 1976.

Brutsaert, W., and M. Parlange, The unstable surface layer above forest—Regional evaporation and heat flux, *Water Resour. Res.*, *28*, 3129–3134, 1992.

Brutsaert, W., and H. Stricker, An advection-aridity approach to estimating actual regional evaporation, *Water Resour. Res.*, *15*, 443–450, 1979.

Brutsaert, W., and M. Sugita, The extent of the unstable Monin-Obukhov layer for temperature and humidity above complex hilly grassland, *Boundary Layer Meteorol.*, *51*, 383–400, 1990.

Brutsaert, W., and M. Sugita, A bulk similarity approach in the atmospheric boundary layer using radiometric skin temperature to determine regional surface fluxes, *Boundary Layer Meteorol.*, *55*, 1–23, 1991.

Brutsaert, W., and M. Sugita, Application of self-preservation in the diurnal evolution of the surface energy budget to determine daily evaporation, *J. Geophys. Res.*, *97*, 18,377–18,382, 1992a.

Brutsaert, W., and M. Sugita, Regional surface fluxes under nonuniform soil moisture conditions during drying, *Water Resour. Res.*, *28*, 1669–1674, 1992b.

Brutsaert, W., and M. Sugita, Regional surface fluxes from satellite-derived surface temperatures (AVHRR) and radiosonde profiles, *Boundary Layer Meteorol.*, *58*, 355–366, 1992c.

Brutsaert, W., M. B. Parlange, and J. H. C. Gash, Neutral humidity profiles in the boundary layer and regional evaporation from sparse pine forest, *Ann. Geophys.*, *7*, 623–630, 1989.

Brutsaert, W., M. Sugita, and L. Fritschen, Inner region humidity characteristics of the neutral boundary layer over prairie terrain, *Water Resour. Res.*, *26*, 2931–2936, 1990.

Burges, S., Trends and directions in hydrology, *Water Resour. Res.*, *22*, suppl., 1S–5S, 1986.

Businger, J. A., J. C. Wyngaard, Y. Izumi, and E. F. Bradley, Flux-profile relationships in the atmospheric surface layer, *J. Atmos. Sci.*, *28*, 181–189, 1971.

Carson, D., Current parameterizations of land-surface processes in atmospheric general circulation models, in *Land Surface Processes in Atmospheric General Circulation Models*, edited by P. Eagleson, pp. 67–108, Cambridge University Press, New York, 1982.

Cheung, T. K., Sodar observations of the stable lower at-

mospheric boundary layer at Barrow, Alaska, *Boundary Layer Meteorol., 57*, 251–274, 1991.

Cheung, T. K., and C. G. Little, Meteorological tower, microbarograph array, and sodar observations of solitary-like waves in the nocturnal boundary layer, *J. Atmos. Sci., 47*, 2516–2536, 1990.

Chou, S., A comparison of airborne eddy correlation and bulk aerodynamic methods for ocean-air turbulent fluxes during cold-air outbreaks, *Boundary Layer Meteorol., 64*, 75–100, 1993.

Choudhury, B. J., Multispectral satellite data in the context of land surface heat balance, *Rev. Geophys., 29*, 217–236, 1991.

Cooney, J., Remote measurements of atmospheric water-vapor profiles using the Raman component of laser back-scatter, *J. Appl. Meteorol., 9*, 182–184, 1970.

Coulter, R., and M. Wesely, Estimates of surface heat flux from sodar and laser scintillation measurements in the unstable boundary layer, *J. Appl. Meteorol., 19*, 1209–1222, 1980.

Crago, R. D., and W. Brutsaert, A comparison of several evaporation equations, *Water Resour. Res., 28*, 951–954, 1992.

Crawford, T., R. McMillen, R. Dobsy, and I. MacPherson, Correction of airborne flux measurements for aircraft speed variation, *Boundary Layer Meteorol., 66*, 237–245, 1993.

Currier, P. E., W. Ecklund, D. Carter, J. Warnock, and B. Balsley, Temperature profiling using a UHF wind profiler and an acoustic source, paper presented at Lower Tropospheric Profiling—Needs and Technologies, Am. Meteorol. Soc., Boston, Mass., May 31 to June 3, 1988.

Dahlquist, H., A one dimensional wind profile model with stability and eddy viscosity estimations from sodar data, *Boundary Layer Meteorol., 62*, 329–351, 1993.

Deardorff, J. W., Preliminary results from numerical integrations of the unstable planetary boundary layer, *J. Atmos. Sci., 27*, 1209–1211, 1970a.

Deardorff, J. W., Convective velocity and temperature scales for the unstable planetary boundary layer and Rayleigh convection, *J. Atmos. Sci., 27*, 1211–1213, 1970b.

Deardorff, J. W., Numerical investigation of neutral and unstable planetary boundary layers, *J. Atmos. Sci., 29*, 91–115, 1972.

DesJardins, R., J. MacPherson, P. Schuepp, and F. Karanja, An evaluation of aircraft flux measurements of CO_2, water vapor and sensible heat, *Boundary Layer Meteorol., 47*, 55–69, 1989.

Dickinson, R. E., Modeling evapotranspiration for three-dimensional global climate models, in *Climate Processes and Climate Sensitivity, Geophys. Monogr. Ser.*, vol. 29, edited by J. E. Hansen and T. Takahashi, pp. 58–72, AGU, Washington, D. C., 1984.

Dickinson, R. E., A. Henderson-Sellers, and P. J. Kennedy, Biosphere-Atmosphere Transfer Scheme (BATS) Version 1e as coupled to the NCAR Community Climate Model, *Tech. Note TN-387+STR*, Natl. Cent. for Atmos. Res., Boulder, Colo., 1993.

Dornbrack, A., and U. Schumann, Numerical simulation of turbulent convective flow over wavy terrain, *Boundary Layer Meteorol., 65*, 323–355, 1993.

Duncan, M., and P. Schuepp, A method to delineate extreme structures within airborne flux traces over the FIFE site, *J. Geophys. Res., 97*, 18,487–18,498, 1992.

Dyer, A. J., A review of flux-profile relationships, *Boundary Layer Meteorol., 7*, 363–372, 1974.

Eagleson, P. S., Global scale hydrology, *Water Resour. Res., 22*, suppl., 6S–14S, 1986.

Eichinger, W., D. Cooper, D. Holtkamp, R. Karl Jr., J. Moses, C. Quick, and J. Tiee, Derivation of water vapor fluxes from lidar measurements, *Boundary Layer Meteorol., 63*, 39–64, 1993a.

Eichinger, W., D. Cooper, M. Parlange, and G. Katul, The application of a scanning, water-Raman lidar as a probe of the atmospheric boundary layer, *IEEE Trans. Geosci. Remote Sens., 31*(1), 70–79, 1993b.

Eichinger, W., D. Cooper, F. Archuleta, D. Hof, D. Holtkamp, R. Karl Jr., C. Quick, and J. Tiee, Development and application of a scanning, solar-blind water Raman-lidar, *Appl. Opt., 33*, 3923–3932, 1994.

Eilts, M. D., Low altitude wind shear detection with Doppler radar, *J. Clim. Appl. Meteorol., 26*, 96–106, 1987.

Eloranta, E. W., and D. K. Forrest, Volume-imaging lidar observations of the convective structure surrounding the flight path of a flux-measuring aircraft, *J. Geophys. Res., 97*, 18,383–18,393, 1992.

Eloranta, E. W., and J. L. Schols, Measurements of spatially averaged wind profiles with volume imaging lidar, paper presented at Fifteenth International Laser Radar Conference, Tomsk, Russia, July 23–27, 1990.

Englisch, W., and W. Wiesemann, Remote sensing of atmospheric trace gases by differential absorption spectroscopy, in Proceedings International Conference on Earth Observations From Space and Management of Planetary Resources, *Eur. Space Agency Spec. Publ., ESA SP-134*, 465–473, 1978.

Ferguson, J. A., and D. H. Stephens, Algorithm for inverting lidar returns, *Appl. Opt., 22*, 3673–3674, 1983.

Ferziger, J. H., Subgrid-scale modeling, in *Large Eddy Simulation of Complex Engineering and Geophysical Flows*, edited by B. Galperin, and S. A. Orszag, pp. 37–54, Cambridge University Press, New York, 1993.

Foufoula-Georgiou, E., and P. Guttorp, Compatibility of continuous rainfall occurrence models with discrete rainfall observations, *Water Resour. Res., 22*, 1316–1322, 1986.

Frisch, A., and S. Clifford, A study of convection capped by a stable layer using Doppler radar and acoustic echo sounders, *J. Atmos. Sci., 31*, 1622–1628, 1974.

Frisch, U., P. L Sulem, and M. Nelkin, A simple dynamical model of intermittent fully developed turbulence, *J. Fluid Mech., 87*, 719–736, 1978.

Fukao, S., T. Sato, and N. Yamasaki, Winds measured by a UHF Doppler radar and rawinsondes: Comparisons made on twenty-six days at Arecibo, Puerto Rico, *J. Appl. Meteorol., 21*, 1357–1363, 1982.

Galchen, T., M. Xu, and W. L. Eberhard, Estimations of atmospheric boundary layer fluxes and other turbulence parameters from Doppler lidar data, *J. Geophys. Res., 97*, 18,409–18,423, 1992.

Gall, R., D. Perner, and A. Ladstatter-Weissenmayer, Simultaneous determination of NH_3, SO_2, NO, and NO_2 by direct UV-absorption in ambient air, *Fresenius J. Anal. Chem., 340*, 646–649, 1991.

Garnier, A., and M. L. Chanin, Description of a Doppler Rayleigh lidar for measuring winds in the middle atmosphere, *Appl. Phys. B, 55*, 35–40, 1992.

Garratt, J. R., *The Atmospheric Boundary Layer*, 316 pp., Cambridge University Press, New York, 1992.

Gash, J. H. C., W. J. Shuttleworth, C. R. Lloyd, J. C. André, J. P. Goutorbe, and J. Gelpe, Micrometeorological measurements in Les Landes Forest during HAPEX-MOBILHY, *Agric. For. Meteorol., 46*, 131–147, 1989.

Gera, B., and S. Singal, Sodar in air pollution meteorology, *Atmos. Environ., Part A, 24*, 2003–2009, 1990.

Gera, B., and A. Weill, Doppler sodar observations of the boundary-layer parameters and a frontal system during

the Mesogers-84 experiment, *Boundary Layer Meteorol.*, *54*, 41–57, 1990.

Gibson, C., and W. Schwartz, The universal equilibrium spectra of turbulent velocity and scalar fields, *J. Fluid Mech.*, *16*, 365–384, 1963.

Glaser, R. E., N. Dagan, O. Furer, and M. Gamliel, A comparison of balloon soundings and lidar scans for measuring the height of the turbulent mixed layer at a coastal site in Israel, *Water Sci. Technol.*, *27*, 271–278, 1993.

Glooschenko, W. A., N. T. Roulet, L. A. Barrie, H. I. Schiff, and H. G. McAdie, The Northern Wetlands Study (NOWES): An overview, *J. Geophys. Res.*, *99*, 1423–1428, 1994.

Goodrich, D. C., T. J. Schmugge, T. J. Jackson, C. L. Unkrich, T. O. Keefer, R. Parry, L. A. Bach, and S. A. Amer, Runoff simulation sensitivity to remotely sensed initial soil water, *Water Resour. Res.*, *30*, 1393–1405, 1994.

Gossard, E., R. Chadwick, W. Neff, and K. Moran, The use of ground-based Doppler radars to measure gradients, fluxes and structure parameters in elevated layers, *J. Appl. Meteorol.*, *21*, 211–226, 1982.

Goutorbe, J. P., J. Noilhan, C. Valancogne, and R. H. Cuenca, Soil moisture variations during HAPEX-MOBILHY, *Ann. Geophys.*, *7*, 415–425, 1989.

Govindaraju, R. S., and M. L. Kavvas, Modeling the erosion process over steep slopes: Approximate analytical solutions, *J. Hydrol.*, *127*, 279–305, 1991.

Govindaraju, R. S., M. L. Kavvas, and S. E. Jones, Approximate analytical solutions for overland flows, *Water Resour. Res.*, *26*, 2903–2912, 1990.

Graber, W., Sodar monitoring of the atmosphere—Recent developments, *Appl. Phys. B*, *57*, 1–2, 1993.

Granger, R. J., A complementary relationship approach for evaporation from nonsaturated surfaces, *J. Hydrol.*, *111*, 31–38, 1989.

Grant, W., He-Ne and CW CO_2 laser long-path systems for gas detection, *Appl. Opt.*, *25*, 709–719, 1986.

Grant, W., Differential absorption and Raman lidar for water vapor profile measurements—A review, *Opt. Eng.*, *30*, 40–48, 1990.

Grossman, R. L., Temporal variation of heat and moisture flux within the atmospheric boundary layer over a grassland, in *Land Surface Evaporation Measurement and Parameterization*, edited by T. J. Schmugge and J.-C. André, chap. 16, pp. 275–285, Springer-Verlag, New York, 1991.

Grossman, R. L., Convective boundary layer budgets of moisture and sensible heat over an unstressed prairie, *J. Geophys. Res.*, *97*, 18,425–18,438, 1992.

Grund, C. J., and E. W. Eloranta, High repetition rate continuously pumped, injection seeded Nd:YAG laser extends high spectral resolution lidar capabilities, paper presented at conference on Remote Sensing of the Atmosphere, Opt. Soc. of Am., Incline Village, Nev., Feb. 12–15, 1990.

Grund, C. J., and E. W. Eloranta, University of Wisconsin high spectral resolution lidar, *Opt. Eng.*, *30*, 6–12, 1991.

Hacker, J. M., The spatial distribution of the vertical energy fluxes over a desert lake area, *Aust. Meteorol. Mag.*, *36*, 235–243, 1988.

Hadfield, M. G., W. R. Cotton, and R. A. Pielke. Large-eddy simulations of thermally forced circulations in the convective boundary layer, 2, A small-scale circulation with zero wind, *Boundary Layer Meteorol.*, *57*, 79–114, 1991.

Hadfield, M. G., W. R. Cotton, and R. A. Pielke, Large-eddy simulations of thermally forced circulations in the convective boundary layer, 2, The effect of changes in wavelength and wind speed, *Boundary Layer Meteorol.*, *58*, 307–327, 1992.

Hairsine, P., and C. Rose, Modeling water erosion due to overland flow using physical principles, 1, Sheet flow, *Water Resour. Res.*, *28*, 237–243, 1992a.

Hairsine, P., and C. Rose, Modeling water erosion due to overland flow using physical principles, 2, Rill flow, *Water Resour. Res.*, *28*, 245–250, 1992b.

Hashmonay, R., A. Cohen, and U. Dayan, Lidar observation of the atmospheric boundary layer in Jerusalem, *J. Appl. Meteorol.*, *3*, 1228–1236, 1991.

Hechtel, L. M., C.-H. Moeng, and R. B. Stull, The effects of nonhomogeneous surface fluxes on the convective boundary layer: A case study using large-eddy simulation, *J. Atmos. Sci.*, *47*, 1722–1741, 1990.

Henn, D. S., and R. I. Sykes, Large-eddy simulation of dispersion in the convective boundary layer, *Atmos. Environ., Part A*, *26*, 3145–3159, 1992.

Hewlett, J., J. Fortson, and G. Cunningham, The effect of rainfall intensity on storm flow and peak discharge from forest land, *Water Resour. Res.*, *13*, 259–266, 1977.

Hill, R., Comparison of scintillation methods for measuring the inner scale of turbulence, *Appl. Opt.*, *27*, 2187–2193, 1988.

Hill, R., G. Ochs, and J. Wilson, Measuring surface layer fluxes of heat and momentum using optical scintillation, *Boundary Layer Meteorol.*, *58*, 391–408, 1992.

Hinkley, E., R. Ku, and P. Kelley, Techniques for detection of molecular pollutants by absorption of laser radiation, in *Laser Monitoring of the Atmosphere*, edited by E. D. Hinkley, Springer-Verlag, New York, 1976.

Hogstrom, U., Non-dimensional wind and temperature profiles in the atmospheric surface layer: A re-evaluation, *Boundary Layer Meteorol.*, *42*, 55–78, 1988.

Holtslag, A. A. M., and C.-H. Moeng, Eddy diffusivity and countergradient transport in the convective atmospheric boundary layer, *J. Atmos. Sci.*, *48*, 1690–1698, 1991.

Hooper, W., and E. Eloranta, Lidar measurements of wind in the planetary boundary layer: The method, accuracy and results from joint measurements with radiosonde and kytoon, *J. Clim. Appl. Meteorol.*, *25*, 990–1001, 1986.

Hornberger, G. M., P. F. Germann, and K. J. Beven, Throughflow and solute transport in an isolated sloping soil block in a forested catchment, *J. Hydrol.*, *124*, 81–99, 1991.

Humes, K. S., W. P. Kustas, M. S. Moran, W. D. Nichols, and M. A. Weltz, Variability of emissivity and surface temperature over a sparsely vegetated surface, *Water Resour. Res.*, *30*, 1299–1310, 1994.

Ivanova, I. D., L. L. Gurdev, and V. M. Mitev, Lidar technique for simultaneous temperature and pressure measurement based on rotational Raman scattering, *J. Mod. Opt.*, *40*, 367–371, 1993.

Jorgensen, H. E., and T. Mikkelsen, Lidar measurements of plume statistics, *Boundary Layer Meteorol.*, *62*, 361–378, 1993.

Kader, B. A., Three-layer structure of an unstably stratified atmospheric surface layer, *Izv. Acad. Sci. USSR Atmos. Oceanic Phys.*, Engl. Transl., *24*, 907–918, 1988.

Kader, B. A., and V. G. Perepelkin, Effect of unstable stratification on the wind speed and temperature profiles in the surface layer, *Izv. Acad. Sci. USSR Atmos. Oceanic Phys.*, Engl. Transl., *25*, 583–588, 1989.

Kader, B. A., and A. M. Yaglom, Mean fields and fluctuation moments in unstably stratified turbulent boundary layers, *J. Fluid Mech.*, *212*, 637–662, 1990.

Kaimal, J. C., and J. J. Finnigan, *Atmospheric Boundary Layer Flows: Their Structure and Measurement*, 289 pp., Oxford University Press, New York, 1994.

Katul, G. G., and M. B. Parlange, A Penman-Brutsaert model for wet surface evaporation, *Water Resour. Res.*, *28*, 121–126, 1992.

Katul, G. G., and M. B. Parlange, On the active role of temperature in surface layer turbulence. *J. Atmos. Sci.*, *51*, 2181–2195, 1994.

Katul, G. G., and M. B. Parlange, The spatial structure of turbulence in the dynamic and dynamic-convective sublayers using wavelet transforms, *Boundary Layer Meteorol.*, in press, 1995.

Katul, G. G., J. Albertson, C.-R. Chu, M. Parlange, H. Stricker, and S. Tyler, Sensible and latent heat flux predictions using conditional sampling methods, *Water Resour. Res.*, *30*, 3053–3059, 1994a.

Katul, G. G., M. Parlange, and C.-R. Chu, Intermittency, local isotropy, and non-Gaussian statistics in stratified atmospheric surface layer turbulent flows, *Phys. Fluids*, *6*, 2480–2492, 1994b.

Katul, G. G., J. D. Albertson, M. Parlange, C.-R. Chu, and H. Stricker, Conditional sampling, bursting, and the intermittent structure of sensible heat flux, *J. Geophys. Res.*, *99*, 22,869–22,876, 1994c.

Katz, R. W., Precipitation as a chain-dependent process, *J. Appl. Meteorol.*, *16*, 671–676, 1977a.

Katz, R. W., An application of chain-dependent processes to meteorology, *J. Appl. Probab.*, *14*, 598–603, 1977b.

Katz, R. W., and M. Parlange, Effects of an index of atmospheric circulation on stochastic properties of precipitation, *Water Resour. Res.*, *29*, 2335–2344, 1993.

Katz, R. W., and M. B. Parlange, Generalizations of chain-dependent processes: Application to hourly precipitation, *Water Resour. Res.*, in press, 1995.

Kavvas, M., and Z. Chen, A radar-based stochastic model for the time-space arrivals of the rain fields onto a geographical region, *Stochastic Hydrol. Hydraul.*, *3*, 261–280, 1989.

Kazanskii, A. B., and A. S. Monin, On the dynamical interaction between the atmosphere and the Earth's surface (in Russian), *Izv. Akad. Nauk SSSR Ser. Geofiz.*, *5*, 514–515, 1961.

Killinger, D., N. Menyuk, and W. E. DeFeo, Remote sensing of CO using frequency doubled CO_2 laser radiation, *Appl. Phys. Lett.*, *36*, 402–405, 1980.

Klett, J. D., Stable analytical inversion solution for processing lidar returns, *Appl. Opt.*, *20*, 1638–1647, 1981.

Klett, J. D., Lidar inversion with variable backscatter/extinction ratios, *Appl. Opt.*, *24*, 1609–1624, 1985.

Killinger, D. K., and N. Menyuk, Remote probing of the atmosphere using a CO_2 DIAL system, *IEEE J. Quantum Electron.*, *QE-17*, 1917–1929, 1981.

Kohsiek, W., Observation of the structure parameters C_t^2, C_{tq} and C_q^2 in the mixed layer over land, *Appl. Opt.*, *27*, 2236–2239, 1988.

Kolev, I., O. Parvanov, and B. Kaprielov, Lidar determination of winds by aerosol inhomogeneities: Motion velocity in the planetary boundary layer, *Appl. Opt.*, *27*, 2524–2531, 1988.

Kolmogorov, A. N., The local structure of turbulence in incompressible viscous fluid for very large Reynolds numbers (in Russian), *Dokl. Akad. Nauk SSSR*, *4*, 299–303, 1941.

Kolmogorov, A. N., A refinement of previous hypotheses concerning the local structure of turbulence in a viscous incompressible fluid at high Reynolds number, *J. Fluid Mech.*, *13*, 82–85, 1962.

Kormakov, A., L. Kosovskii, N. Kurochkin, and G. Pogosov, Comparing wind speed vector meters—Doppler lidar and meteorological mast, *Meas. Tech.*, Engl. Transl., *36*, 548–550, 1993.

Kraichnan, R. H., Turbulent cascade and intermittency growth, *Proc. R. Soc. London A*, *434*, 65–78, 1991.

Kunkel, K., E. Eloranta, and J. Weinman, Remote determination of winds, turbulence spectra and energy dissipation rates in the boundary layer from lidar measurements, *J. Atmos. Sci.*, *37*, 978–985, 1980.

Kustas, W. P., and W. Brutsaert, Wind profile constants in a neutral atmospheric boundary layer over complex terrain, *Boundary Layer Meteorol.*, *34*, 33–54, 1986.

Kustas, W. P., and W. Brutsaert, Budgets of water vapor in the unstable boundary layer over rugged terrain, *J. Clim. Appl. Meteorol.*, *26*, 607–620, 1987.

Kustas, W. P., and D. C. Goodrich, Preface to special section: Monsoon '90 multidisciplinary experiment, *Water Resour. Res.*, *30*, 1211–1225, 1994.

Landau, L. D., and E. M. Lifshitz, *Fluid Mechanics*, 536 pp., Pergamon, New York, 1959.

Lenschow, D., E. Miller, and R. B. Friesen, A 3-aircraft intercomparison of 2 types of air motion measurement systems, *J. Atmos. Oceanic Technol.*, *8*, 41–50, 1991.

Lenschow, D. H., J. Mann, and L. Kristensen, How long is long enough when measuring fluxes and other turbulence statistics?, *J. Atmos. Oceanic Technol.*, *11*, 661–673, 1994.

Leonard, A., Energy cascade in large-eddy simulations of turbulent fluid flows, *Adv. Geophys.*, *18A*, 237–249, 1974.

Lindroth, A., Gradient distributions and flux profile relations above a rough forest, *Q. J. R. Meteorol. Soc.*, *110*, 553–563, 1984.

Little, C., Acoustic methods for the remote probing of the lower atmosphere, *Proc. IEEE*, *57*, 571–578, 1969.

Loague, K., and R. Freeze, A comparison of rainfall-runoff modeling techniques on small upland catchments, *Water Resour. Res.*, *21*, 229–248, 1985.

MacPherson, J., R. Grossmann, and R. Kelly, Intercomparison and results from FIFE flux aircraft, *J. Geophys. Res.*, *97*, 18,499–18,514, 1992.

Mahrt, L., Mixed layer moisture structure, *Mon. Weather Rev.*, *104*, 1403–1407, 1976.

Mahrt, L., Intermittency of atmospheric turbulence, *J. Atmos. Sci.*, *46*, 79–95, 1989.

Mahrt, L., and M. Ek, Spatial variability of turbulent fluxes and roughness lengths in HAPEX-MOBILHY, *Boundary Layer Meteorol.*, *65*, 381–400, 1993.

Mann, J., and D. H. Lenschow, Errors in airborne flux measurements, *J. Geophys. Res.*, *99*, 14,519–14,526, 1994.

Mason, P. J., Large-eddy simulation of the convective atmospheric boundary layer, *J. Atmos. Sci.*, *46*, 1492–1516, 1989.

Mason, P. J., Large-eddy simulation of dispersion in convective boundary layers with wind shear, *Atmos. Environ., Part A*, *26*, 1561–1571, 1992.

Mason, P. J., Large-eddy simulation: A critical review of the technique, *Q. J. R. Meteorol. Soc.*, *120*, 1–26, 1994.

Mason, P. J., and S. H. Derbyshire, Large-eddy simulation of the stably-stratified atmospheric boundary layer, *Boundary Layer Meteorol.*, *53*, 117–162, 1990.

Mason, P. J., and D. J. Thomson, Large-eddy simulations of the neutral-static-stability planetary boundary layer, *Q. J. R. Meteorol. Soc.*, *113*, 413–443, 1987.

May, P., R. Strauch, K. Moran, and W. Ecklund, Temperature sounding by RASS with wind profiler radars: A preliminary study, *IEEE Trans. Geosci. Remote Sens.*, *28*, 19–28, 1990.

Mayer, A., J. Comera, H. Charpentier, and C. Jaussaud, Absorption coefficients of various polllutant gasses at CO_2 laser wavelengths, *Appl. Opt.*, *17*, 391–393, 1978.

McComb, W. D., *The Physics of Fluid Turbulence*, 572 pp., Oxford University Press, New York, 1990.

McDermid, I. S., A 4-year climatology of stratospheric ozone from lidar measurements at Table Mountain, 34.4°N, *J. Geophys. Res.*, *98*, 10,509–10,515, 1993.

Measures, R., *Laser Remote Sensing, Fundamentals and Application*, 510 pp., Wiley-Interscience, New York, 1984.

Measures, R., *Laser Remote Chemical Analysis*, 546 pp., John Wiley, New York, 1988.

Melas, D., Sodar estimates of surface heat flux and mixed layer depth compared with direct measurements, *Atmos. Environ., Part A*, *24*, 2847–2853, 1990.

Melas, D., Similarity methods to derive turbulence quantities and mixed-layer depth from sodar measurements in the convective boundary layer—A review, *Appl. Phys. B*, *57*, 11–17, 1993.

Melfi, S. H., J. D. Lawrence, and M. P. McCormick, Observation of Raman scattering by water-vapor in the atmosphere, *Appl. Phys. Lett.*, *15*, 295–297, 1969.

Melfi, S. H., D. Whiteman, and R. Ferrare, Observation of atmospheric fronts using Raman lidar moisture measurements, *J. Appl. Meteorol.*, *28*, 789–806, 1989.

Meneveau, C., and K. R. Sreenivasan, Simple multifractal cascade model for fully developed turbulence, *Phys. Rev. Lett.*, *59*, 1427–1427, 1987.

Meneveau, C., and K. R. Sreenivasan, The multifractal nature of turbulent energy dissipation, *J. Fluid Mech.*, *224*, 429–484, 1991.

Menyuk, N., D. K. Killinger, and W. E. DeFeo, Remote sensing of NO using a differential absorption lidar, *Appl. Opt.*, *19*, 3282–3286, 1980.

Menyuk, N., D. K. Killinger, and W. E. DeFeo, Laser remote sensing of hydrazine, MMH and UDMH using a differential absorption CO_2 lidar, *Appl. Opt.*, *21*, 2275–2286, 1982.

Milton, M., P. Woods, B. Jolliffe, N. Swann, and T. McIlveen, Measurements of toluene and other aromatic hydrocarbons by differential absorption lidar in the near-ultraviolet, *Appl. Phys B.*, *55*, 41–45, 1992.

Mitev, V. M., I. V. Grigorov, and V. B. Simeonov, Lidar measurements of atmospheric aerosol extinction profiles: A comparison between two techniques—Klett inversion and pure rotational Raman scattering methods, *Appl. Opt.*, *31*, 6469–6474, 1992.

Moeng, C.-H., A large-eddy-simulation model for the study of planetary boundary-layer turbulence, *J. Atmos. Sci.*, *41*, 2052–2062, 1984.

Moeng, C.-H., and J. C. Wyngaard, Statistics of conservative scalars in the convective boundary layer, *J. Atmos. Sci.*, *41*, 3161–3169, 1984.

Moeng, C.-H., and J. C. Wyngaard, Evaluation of turbulent transport and dissipation closures in second-order modeling, *J. Atmos. Sci.*, *46*, 2311–2330, 1989.

Monin, A. S., and A. M. Obukhov, Basic laws of turbulent mixing in the ground layer of the atmosphere (in Russian), *Tr. Geofiz. Inst. Akad. Nauk SSSR*, *151*, 163–187, 1954.

Monteith, J. L., Evaporation and environment, *Symp. Soc. Exp. Biol.*, *19*, 205–234, 1965.

Morton, F. I., Operational estimates of areal evapotranspiration and their significance to the science and practice of hydrology, *J. Hydrol.*, *66*, 1–76, 1983.

Mulders, J. M., Algorithm for inverting lidar returns: Comment., *Appl. Opt.*, *23*, 2855–2856, 1984.

Nedeljkovic, D., A. Hauchecorne, and M. Chanin, Rotational Raman lidar to measure the atmospheric temperature from the ground to 30 km, *IEEE Trans. Geosci. Remote Sens.*, *31*, 90–101, 1993.

Nichols, W. E., and R. H. Cuenca, Evaluation of the evaporative fraction for parameterization of the surface energy balance, *Water Resour. Res.*, *29*, 3681–3690, 1993.

Nielsen, D., J. Biggar, and K. Erh, Spatial variability of field-measured soil-water properties, *Hilgardia*, *42*, 215–259, 1973.

Nieuwstadt, F. T. M., A large-eddy simulation of a line source in a convective atmospheric boundary layer, I, dispersion characteristics, *Atmos. Environ., Part A*, *26*, 485–495, 1992a.

Nieuwstadt, F. T. M., A large-eddy simulation of a line source in a convective atmospheric boundary layer, II, dynamics of a buoyant line source, *Atmos. Environ., Part A*, *26*, 497–503, 1992b.

Noilhan, J., and S. Planton, A simple parameterization of land surface processes for meteorological models, *Mon. Weather Rev.*, *117*, 536–549, 1989.

Noilhan, J., J. C. André, P. Bougeault, J. P. Goutorbe et al., Some aspects of the HAPEX-MOBILHY Programme—The data base and the modelling strategy, *Surv. Geophys.*, *12*, 31–61, 1991.

Obeysekera, J. T. B., G. Q. Tabois III, and J. D. Salas, On parameter estimation of temporal rainfall models, *Water Resour. Res.*, *23*, 1837–1850, 1987.

Panofsky, H. A., and J. A. Dutton, *Atmospheric Turbulence, Models and Methods for Engineering Applications*, 397 pp., Wiley-Interscience, New York, 1984.

Parlange, J.-Y., Water transport in soils, *Annu. Rev. Fluid Mech.*, *12*, 77–102, 1980.

Parlange, J.-Y., I. G. Lisle, R. D. Braddock, and R. E. Smith, The three-parameter infiltration equation, *Soil Sci.*, *133*(6), 337–340, 1982.

Parlange, M., and W. Brutsaert, Regional roughness of the landes forest and surface shear stress under neutral conditions, *Boundary Layer Meteorol.*, *48*, 69–81, 1989.

Parlange, M. B., and W. Brutsaert, Are radiosonde time scales appropriate to characterize boundary layer wind profiles?, *J. Appl. Meteorol.*, *29*, 249–255, 1990.

Parlange, M. B., and W. Brutsaert, Regional shear stress of broken forest from radiosonde wind profiles in the unstable surface layer, *Boundary Layer Meteorol.*, *64*, 355–368, 1993.

Parlange, M. B., and G. G. Katul, An advection-aridity evaporation model, *Water Resour. Res.*, *28*, 127–132, 1992a.

Parlange, M. B., and G. G. Katul, Estimation of the diurnal variation of potential evaporation from a wet bare surface, *J. Hydrol.*, *132*, 71–89, 1992b.

Parlange, M. B., and G. G. Katul, Watershed scale shear stress from tethersonde wind profile measurements under near neutral and unstable atmospheric stability, *Water Resour. Res.*, in press, 1995.

Parlange, M. B., T. S. Steenhuis, D. J. Timlin, F. Stagnitti, and R. B. Bryant, Subsurface flow above a fragipan horizon, *Soil Sci.*, *148*, 77–86, 1989.

Parlange, M. B., G. G. Katul, R. H. Cuenca, M. L. Kavvas, D. R. Nielsen, and M. Mata, Physical basis for a time series model of soil water content, *Water Resour. Res.*, *28*, 2437–2446, 1992a.

Parlange, M. B., S. N. Prasad, J.-Y. Parlange, and M. J. M. Romkens, Extension of the Heaslet-Alksne technique to arbitrary soil-water diffusivities, *Water Resour. Res.*, *28*, 2793–2798, 1992b.

Parlange, M. B., G. G. Katul, M. V. Folegatti, and D. R. Nielsen, Evaporation and the field scale diffusivity function, *Water Resour. Res.*, *29*, 1279–1286, 1993a.

Parlange, M. B., C. Fuentes, R. Haverkamp, J.-Y. Parlange, D. Elrick, and M. J. Price, Optimal solutions of the Bruce and Klute equations, *Soil Sci.*, *155*, 1–7, 1993b.

Pekour, M., and M. Kallistratova, Sodar study of the bound-

ary layer over Moscow for air-pollution application, *Appl. Phys. B*, *57*, 9–55, 1993.

Penmann, H. L., Natural evaporation from open water, bare soil, and grass, *Proc. R. Soc. London A*, *193*, 120–145, 1948.

Priestly, C. H. B., and R. J. Taylor, On the assessment of surface heat flux and evaporation, *Mon. Weather Rev.*, *106*, 81–92, 1972.

Qualls, R. J., W. Brutsaert, and W. P. Kustas, Near-surface air temperature as substitute for skin temperature in regional surface flux estimation, *J. Hydrol.*, *143*, 381–393, 1993.

Quintarelli, F., Acoustic sounder observations of atmospheric turbulence parameters in a convective boundary layer, *J. Appl. Meteorol.*, *32*, 1433–1440, 1993.

Ralph, F., C. Mazaudier, M. Crochet, and S. Venkateswaran, Doppler sodar and radar wind-profiler observations of gravity-wave activity associated with a gravity current, *Mon. Weather Rev.*, *121*, 444–463, 1993.

Rodriguez-Iturbe, I., B. Febres de Power, and J. B. Valdes, Rectangular pulse point process models for rainfall: Analysis of empirical data, *J. Geophys. Res.*, *92*, 9645–9656, 1987.

Rogallo, R. S., and P. Moin, Numerical simulation of turbulent flows, *Annu. Rev. Fluid Mech.*, *16*, 99–137, 1984.

Russchenberg, H., Doppler polarimeter radar measurements of the gamma drop size distribution of rain, *J. Appl. Meteorol.*, *32*, 1815–1825, 1993.

Sanford, W. E., J.-Y. Parlange, and T. S. Steenhuis, Hillslope drainage with sudden drawdown: Closed form solution and laboratory experiments, *Water Resour. Res.*, *29*, 2313–2321, 1993.

Sasano, Y., H. Hirohara, T. Yamasaki, H. Shimizu, N. Takeuchi, and T. Kawamura, Horizontal wind vector determination from the displacement of aerosol distribution patterns observed by a scanning lidar, *J. Appl. Meteorol.*, *21*, 1516–1523, 1986.

Schmidt, H., and U. Schumann, Coherent structures of the convective boundary layer derived from large-eddy simulations, *J. Fluid Mech.*, *200*, 511–562, 1989.

Schmugge, T., T. J. Jackson, W. P. Kustas, R. Roberts, R. Parry, D. C. Goodrich, S. A. Amer, and M. A. Weltz, Push broom microwave radiometer observations of surface soil moisture in Monsoon '90, *Water Resour. Res.*, *30*, 1321–1327, 1994.

Schols, J. L., and E. W. Eloranta, Calculation of area-averaged vertical profiles of the horizontal wind velocity from volume-imaging lidar data, *J. Geophys. Res.*, *97*, 18,395–18,407, 1992.

Schuepp, P., M. Leclerc, J. Macpherson, and R. Desjardins, Footprint prediction of scalar fluxes from analytical solutions of the diffusion equation, *Boundary Layer Meteorol.*, *50*, 353–373, 1990.

Schuepp, P., J. Macpherson, and R. Desjardins, Adjustment of footprint correction for airborne flux mapping over the FIFE site, *J. Geophys. Res.*, *97*, 18,455–18,466, 1992.

Schumann, U., Large-eddy simulation of turbulent diffusion with chemical reactions in the convective boundary layer, *Atmos. Environ., Part A*, *23*, 1713–1727, 1989.

Schumann, U., Large-eddy simulation of the up-slope boundary layer, *Q. J. R. Meteorol. Soc.*, *116*, 637–670, 1990.

Schumann, U., Large eddy simulation of turbulent convection over flat and wavy surfaces, in *Large Eddy Simulation of Complex Engineering and Geophysical Flows*, edited by B. Galperin and S. A. Orszag, pp. 399–421, Cambridge University Press, New York, 1993.

Scott, S., T. Bui, K. Chan, and S. Bowen, The meteorological measurement system on the NASA ER-2 aircraft, *J. Atmos. Oceanic Technol.*, *7*, 525–540, 1990.

Sellers, P. J., Y. Mintz, Y. C. Sud, and A. Dalcher, A simple biosphere model (SiB) for use within general circulation models, *J. Atmos. Sci.*, *43*, 505–531, 1986.

Sellers, P. J., F. G. Hall, G. Asrar, D. E. Strebel, and R. E. Murphy, An overview of the First International Satellite Land Surface Climatology Project (ISLSCP) Field Experiment (FIFE), *J. Geophys. Res.*, *97*, 18,354–18,371, 1992.

Seth, A., F. Giorgi, and R. E. Dickinson, Simulating fluxes from heterogeneous land surfaces: An explicit subgrid method employing the Biosphere-Atmosphere Transfer Scheme (VBATS), *J. Geophys. Res.*, *99*, 18,651–18,667, 1994.

Shaw, R. H., and U. Schumann, Large-eddy simulation of turbulent flow above and within a forest, *Boundary Layer Meteorol.*, *61*, 47–64, 1992.

Shaw, R. H., W. Gao, and K. T. Paw U, Detection of temperature ramps and flow structures at a deciduous forest site, *Agric. For. Meteorol.*, *47*, 123–138, 1989.

Singal, S., Monitoring air pollution related meteorology using sodar—State of the art, *Appl. Phys. B*, *57*, 65–82, 1993.

Skukla, J., and Y. Mintz, Influence of land-surface evapotranspiration on the Earth's surface climate, *Science*, *215*, 1498–1501, 1982.

Slatyer, R. O., and I. C. McIlroy, *Practical Microclimatology*, 310 pp., Commonwealth Scientific, Industrial, and Research Organisation, Melbourne, Australia, 1967.

Smagorinsky, J., General circulation experiments with the primitive equations, 1, The basic experiment, *Mon. Weather Rev.*, *91*, 99–164, 1963.

Smith, J. A., Statistical modeling of daily rainfall occurrences, *Water Resour. Res.*, *23*, 885–893, 1987.

Sorbjan, Z., *Structure of the Atmospheric Boundary Layer*, 317 pp., Prentice Hall, Englewood Cliffs, N. J., 1989.

Sorbjan, Z., R. L. Coulter, and M. L. Wesley, Similarity scaling applied to sodar observations of the convective boundary layer above an irregular hill, *Boundary Layer Meteorol.*, *56*, 33–50, 1991.

Sroga, J., and E. Eloranta, Lidar measurement of wind velocity profiles in the boundary layer, *J. Appl. Meteorol.*, *19*, 598–605, 1980.

Stagnitti, F., J.-Y. Parlange, T. S. Steenhuis, M. B. Parlange, and C. W. Rose, A mathematical model of hillslope and watershed discharge, *Water Resour. Res.*, *28*, 2111–2122, 1992.

Stannard, D. I., J. H. Blanford, W. P. Kustas, W. D. Nichols, S. A. Amer, T. J. Schmugge, and M. A. Weltz, Interpretations of surface flux measurements in heterogeneous terrain during Monsoon '90, *Water Resour. Res.*, *30*, 1227–1239, 1994.

Stricker, H., and W. Brutsaert, Actual evaporation over a summer period in the Hupsel Catchment, *J. Hydrol.*, *39*, 139–157, 1978.

Stull, R., The energetics of entrainment across a density interface, *J. Atmos. Sci.*, *33*, 1260–1267, 1976.

Stull, R., *An Introduction to Boundary Layer Meteorology*, 666 pp., Kluwer Academic, Norwell, Mass., 1988.

Sugita, M., and W. Brutsaert, Regional surface fluxes from remotely sensed skin temperature and lower boundary layer measurements, *Water Resour. Res.*, *26*, 2937–2944, 1990a.

Sugita, M., and W. Brutsaert, Wind velocity measurements in the neutral boundary layer above hilly prairie, *J. Geophys. Res.*, *95*, 7617–7624, 1990b.

Sugita, M., and W. Brutsaert, Daily evaporation over a region from lower boundary layer profiles measured with radiosondes, *Water Resour. Res.*, *27*, 747–752, 1991.

Sugita, M., and W. Brutsaert, The stability functions in the bulk similarity formulation for the unstable boundary layer, *Boundary Layer Meteorol.*, *61*, 65–80, 1992a.

Sugita, M., and W. Brutsaert, Landsat surface temperatures and radio soundings to obtain regional surface fluxes, *Water Resour. Res.*, *28*, 1675–1679, 1992b.

Suto, M., X. Wang, J. Shan, and L. Lee, Quantitative photoabsorption and fluorescence spectroscopy of benzene, naphthalene, and some derivatives at 106–295 nm., *J. Quant. Spectrosc. Radiat. Transfer*, *48*, 79–89, 1992.

Sykes, R. I., and D. S. Henn, Large-eddy simulation of concentration fluctuations in a dispersing plume, *Atmos. Environ., Part A*, *26*, 3127–3144, 1992.

Sykes, R. I., D. S. Henn, S. F. Parker, and W. S. Lewellen, Large eddy simulation of a turbulent reacting plume, *Atmos. Environ., Part A*, *26*, 2565–2574, 1992.

Sykes, R. I., D. S. Henn, and W. S. Lewellen, Surface-layer description under free-convection conditions, *Q. J. R. Meteorol. Soc.*, *119*, 409–421, 1993.

Taylor, G. I., The spectrum of turbulence, *Proc. R. Soc. London A*, *164*, 476–490, 1938.

Tennekes, H., Free convection in the turbulent Ekman layer of the atmosphere, *J. Atmos. Sci.*, *27*, 1027–1034, 1970.

Tennekes, H., A model for the dynamics of the inversion above a convective boundary layer, *J. Atmos. Sci.*, *30*, 558–567, 1973.

Tennekes, H., and J. Lumley, *A First Course in Turbulence*, 300 pp., MIT Press, Cambridge, Mass., 1972.

Thom, A., Momentum, mass and heat exchange of vegetation, *Q. J. R. Meteorol. Soc.*, *97*, 414–428, 1972.

Thomas, P., and S. Vogt, Intercomparison of turbulence data measured by sodar and sonic anemometers, *Boundary Layer Meteorology*, *62*, 353–359, 1993a.

Thomas, P., and S. Vogt, Variances of the vertical and horizontal wind measured by tower instruments and sodar—An intercomparison, *Appl. Phys. B*, *57*, 19–26, 1993b.

Todorovic, P., and D. A. Woolhiser, A stochastic model of *n*-day precipitation, *J. Appl. Meteorol.*, *14*, 17–24, 1975.

Troch, P. A., F. P. De Troch, and W. Brutsaert, Effective water table depth to describe initial conditions prior to storm rainfall in humid regions, *Water Resour. Res.*, *29*, 427–434, 1993.

Tsvang, L., M. Fedorov, B. Kader, and S. Zubkovskii, Turbulent exchange over a surface with chessboard-type inhomogeneities, *Boundary Layer Meteorol.*, *55*, 141–160, 1991.

Uthe, E., Airborne CO_2 dial measurement of atmospheric tracer gas concentration distributions, *Appl. Opt.*, *25*, 2492–2498, 1986.

Vandervaere, J. P., M. Vauclin, R. Haverkamp, and R. H. Cuenca, Error analysis in estimating soil water balance of irrigated fields during the EFEDA experiment, 1, Local standpoint, *J. Hydrol.*, *156*, 351–370, 1994.

van Haren, L., and F. T. M. Nieuwstadt, The behavior of passive and buoyant plumes in a convective boundary layer as simulated with a large-eddy model, *J. Appl. Meteorol.*, *28*, 818–832, 1989.

van Haren, L., and F. T. M. Nieuwstadt, A large-eddy simulation of buoyant plumes in a convective boundary layer, *Nuovo Cimento*, *13*, 923–931, 1990.

Vaughn, G., D. P. Wareing, L. Thomas, and V. Mitev, Humidity measurements in the free troposphere using Raman backscatter, *Q. J. R. Meteorol. Soc.*, *114*, 1471–1484, 1988.

Walko, R. L., W. R. Cotton, and R. A. Pielke, Large-eddy simulations of the effects of hilly terrain on the convective boundary layer, *Boundary Layer Meteorol.*, *58*, 133–150, 1992.

Warnock, J., T. VanZandt, J. Green, and R. Winkler, Comparison between wind profiles measured by Doppler radar and by rawinsonde balloons, *Geophys. Res. Lett.*, *5*, 109–112, 1978.

Wendt, J. F. (Ed.), *Computational Fluid Dynamics: An Introduction*, 291 pp., Springer-Verlag, New York, 1992.

Whiteman, D. N., S. H. Melfi, and R. A. Ferrare, Raman lidar system for the measurement of water vapor and aerosols in the Earth's atmosphere, *Appl. Opt.*, *31*, 3068–3082, 1992.

Wieringa, J., Representative roughness parameters for homogeneous terrain, *Boundary Layer Meteorol.*, *63*, 323–363, 1993.

Wilks, D. S., Comparison of three-parameter probability distributions for representing annual extreme and partial duration precipitation series, *Water Resour. Res.*, *29*, 3543–3549, 1993.

Wilson, D., Doppler radar studies of boundary layer wind profiles and turbulence in snow conditions, in *Proceedings of the 14th Conference on Radar Meteorology*, pp. 616–623, American Meteorological Society, Boston, Mass., 1970.

Wood, E. F., Global scale hydrology: Advances in land surface modeling, *U.S. Natl. Rep. Int. Union Geod. Geophys. 1987–1990*, *Rev. Geophys.*, *29*, 193–201, 1991.

Wood, E. F., M. Sivapalan, and K. Beven, Similarity and scale in catchment storm response, *Rev. Geophys.*, *28*, 1–18, 1990.

Woolhiser, D. A., T. O. Keefer, and K. T. Redmond, Southern oscillation effects on daily precipitation in the southwestern United States, *Water Resour. Res.*, *29*, 1287–1295, 1993.

Wyngaard, J. C., and R. A. Brost, Top-down and bottom-up diffusion of a scalar in the convective boundary layer, *J. Atmos. Sci.*, *41*, 102–112, 1984.

Wyngaard, J. C., W. T. Pennell, D. H. Lenschow, and M. A. LeMone, The temperature-humidity covariance budget in the convective boundary layer, *J. Atmos. Sci.*, *41*, 1959–1969, 1984.

Yaglom, A. M., Comments on wind and temperature flux-profile relationships, *Boundary Layer Meteorol.*, *11*, 89–102, 1977.

Yamada, T., On the similarity functions A, B, and C of the planetary boundary layer, *J. Atmos. Sci.*, *33*, 781–793, 1976.

Zecharias, Y. B., and W. Brutsaert, Recession characteristics of groundwater outflow and baseflow from mountainous watersheds, *Water Resour. Res.*, *24*, 1651–1658, 1988.

Zilitinkevich, S. S., On the turbulence and diffusion under free convection conditions (in Russian), *Izv. Akad. Nauk. SSSR Fiz. Atmos. Okeana*, *7*, 1263–1269, 1971.

Zilitinkevich, S. S., and J. W. Deardorff, Similarity theory for the planetary boundary layer of time-dependent height, *J. Atmos. Sci.*, *31*, 1449–1452, 1974.

J. D. Albertson, W. E. Eichinger, and M. B. Parlange, Hydrologic Science, University of California, Davis, CA 95616.